Structural investigations of paramagnetic metalloproteins using high-resolution NMR spectroscopy: iron-sulfur and copper proteins

A. I. Dikiy

*Department of Agro-Environmental Science and Technology, University of Bologna, 8 Via Filippo Re, I-40127 Bologna, Italy.**
Fax: +39 051 2099792. E-mail: dikiy@cerm.unifi.it

Current approaches to the structural investigations of paramagnetic metal-containing proteins in solution using NMR spectroscopy are surveyed taking iron-sulfur and copper-containing proteins as examples.

Key words: NMR, paramagnetic metalloproteins, protein structure in solution, electronic structure.

Introduction

An important task of modern biochemistry is determination of the spatial structures and study of the structural and functional characteristics of proteins. The topicality of this task increased when studies on determination of the genomes of some organisms** had resulted in the discovery of many new proteins. The functions of most of them are unknown. An important step in elucidating the role of proteins in biological processes is determination of their three-dimensional structures.

The most important data on the 3D structures of biological macromolecules are provided by X-ray diffraction analysis and high-resolution NMR spectroscopy. These methods permit one to determine the spatial structures of proteins, to compare the molecular conformations in the crystal and in solution, and to elucidate the structural features determining the functional properties of a system.

NMR spectroscopy is a powerful and, to a large extent, unique tool of structural biology, which makes it possible to study a system under conditions close to physiological conditions. This technique provides structural information at the atomic level of resolution, allows one to judge the dynamics of macromolecules in solution, and makes it possible to describe the properties of proteins that are disordered completely or partially.[1,2]

NMR spectroscopy was first employed in 1985 to elucidate the structure of a protein in solution.[3] Further development of the theoretical grounds of this method[4,5—8] and elaboration of new techniques[9,10] ensured substantial progress in the structural investigation of diamagnetic proteins. Enrichment of proteins in ^{15}N, ^{13}C, and ^{2}H isotopes and the use of advanced sequences of NMR pulses make it possible to work with proteins with high molecular masses (up to 40 kDa).[1,2,11—14]

Specific features of NMR spectroscopy of paramagnetic metal-containing systems

The active sites of many proteins contain metal ions. The paramagnetic state of these ions is often biologically significant. Whereas the determination of 3D structures for diamagnetic proteins is a well developed and extensively used procedure,[1,15] the procedures for working with paramagnetic metalloproteins are at the stage of intense development and design.[16—19] Indeed, at present, the overwhelming majority of protein structures determined by NMR and deposited at the protein structure data bank* (PDB) correspond to diamagnetic proteins. The difficulties involved in the work with paramagnetic proteins are due to the presence of unpaired electrons in the system. The interaction of electrons with nuclear spins induces substantial changes in the nuclear chemical shifts, increases the rates of nuclear relaxation (spin—lattice, T_1**, and spin—spin, T_2***).[20—22] The increase in the rate of spin—lattice relaxation complicates the detection of dipole interactions between the nuclei and thus hampers gaining of data on the structure of the system under study. The increase in the rate of spin—spin relaxation results in signal broadening and thus hampers the detection of signals in the NMR spectra, which also leads to a loss of structural information.

* Dipartipento di Scienze Tecnologiche e Agro-Ambientali, Universitá di Bologna, 8 via Filippo Re, I-40127 Bologna, Italy.
** See http://www.ncbi.nlm.nih.gov.

* See http://www.rcsb.org.
** Longitudinal relaxation time.
*** Transverse relaxation time.

Published in Russian in *Izvestiya Akademii Nauk. Seriya Khimicheskaya,* No. 10, pp. 1680—1705, October, 2001.

1066-5285/01/5010-1762 $25.00

The interaction of nuclei with unpaired electrons can follow different mechanisms, namely, the contact (Fermi) mechanism,[23,24] consisting in the interaction between the electronic and nuclear momenta through a chemical bond, the pseudo-contact (dipole) mechanism,[25] which is through-space interaction, and the Curie mechanism,[26,27] based on the interaction between the nucleus and the electronic magnetic moment arising due to different occupancies of the electronic energy levels in the metal atom. The two first-mentioned mechanisms contribute to both the observed chemical shift and the rate of nuclear relaxation, while the last one affects only the rate of transverse relaxation ($1/T_2$). The paramagnetic interaction can involve both the nuclei of amino acids that are coordinated directly to the paramagnetic metal ion and the nuclei of the residues located at a certain distance from the metal ion. The radius of the sphere of ion influence can reach 30—40 Å.[28] The extent to which unpaired electrons influence the spectral parameters as well as the specific contributions of different mechanisms to the interaction of the unpaired electron with the nucleus depend on the nature of the metal ion.

The electron relaxation in the metal ion occurs due to the spin—orbit interaction and depends on the distribution of the energy levels, which, in turn, depends on the number of ligands at the metal ion and its coordination geometry.[29] The electron relaxation time in a metal ion is an important parameter characterizing the effect of the unpaired electron on the spectral characteristics of the system. It is generally accepted[30] that the signals of protons located in the close proximity to the paramagnetic center can be detected in the ^{1}H NMR spectrum provided that the time of electron relaxation in the metal ion is shorter than 10^{-11} s. The electron relaxation rates for various metal ions at room temperature and the corresponding signal widths for the proton located at a distance of 5 Å from the metal ion in a 11.7 T magnetic field are listed[31] in Table 1.

Systems containing an iron ion are the most convenient for NMR investigation (see Table 1). For example, cytochromes,[32,33] peroxidases and their derivatives,[34—37] and myoglobine and its derivatives[38—41] have been studied. Owing to the magnetic interaction between metal ions, the proteins containing bimetallic or polymetallic centers can also be studied by NMR spectroscopy. When a rapidly relaxing ion interacts with a slowly relaxing one, the electron relaxation rate in the latter increases because it utilizes relaxation mechanisms of the rapidly relaxing ion. Depending on the strength of the electron—electron interaction, the relaxation rate of the slowly relaxing ion can increase to reach the relaxation rate of the rapidly relaxing ion. This results in much narrower signals of the ligand nuclei for the slowly relaxing metal ion, which enables and facilitates investigation of this system by NMR.[22,42] This type of interaction is observed in a number of biologically important systems: Cu^{II}—Co^{II} (superoxide dismutase),[43,44] Fe^{III}—Fe^{II} (iron-sulfur proteins,[45—47] phosphatases[48,49]), Cu^{II}—Cu^{I} (the Cu_A-domain cytochrome *c*-oxidase),[50—54] *etc.*

Table 1. Electron relaxation time for paramagnetic metal ions and corresponding signal broadening for the protons located at 5 Å distance from the metal ion in a 11.7 T magnetic field

Ion	τ_e/s^{-1}	Line broadening/Hz
Ti^{3+}	10^{-10}—10^{-11}	20—200
VO^{2+}	10^{-8}	10000
V^{3+}	10^{-11}	50
V^{2+}	10^{-9}	5000
Cr^{3+}	$5\cdot10^{-9}$—$5\cdot10^{-10}$	3000—25000
Cr^{2+}	10^{-11}—10^{-12}	20—150
Mn^{3+}	10^{-10}—10^{-11}	150—1500
Mn^{2+}	10^{-8}	100000
Fe^{3+} (HS)	10^{-9}—10^{-11}	200—12000
Fe^{3+} (LS)	10^{-11}—10^{-13}	0.5—20
Fe^{2+} (HS)	10^{-11}—10^{-13}	5—150
Co^{2+} (HS)	10^{-11}—10^{-13}	2—100
Co^{2+} (LS)	10^{-9}—10^{-10}	200—1000
Ni^{2+}	10^{-10}—10^{-12}	5—500
Cu^{2+}	10^{-9}	1000—5000
Ru^{3+}	10^{-11}—10^{-12}	2—20
Re^{3+}	10^{-12}—10^{-13}	5—20
Gd^{3+}	10^{-8}—10^{-9}	20000—200000
Ln^{3+}	10^{-12}—10^{-13}	1—100

Note. HS is the high-spin form, LS is the low-spin form. Line broadening is assumed to be due to the dipole interaction of the nucleus with the unpaired electron. The correlation time for this interaction is determined by the electron relaxation time.[31]

Two approaches are possible to the structural study of paramagnetic proteins using NMR spectroscopy: (1) determination of the full 3D structure of a protein, and (2) study of the structure of the protein active site.

As noted above, a paramagnetic center prevents or, at least, markedly complicates the procedure of determination of the 3D structure of a molecule. From this standpoint, the presence of unpaired electrons is an obvious "disadvantage" of the system. However, the interaction of the unpaired electron with the surrounding nuclei makes it possible to elucidate the structural constraints supplementing those used for diamagnetic systems, which are useful in the calculations of the three-dimensional structure of the protein. The distance and angle constraints can be found by analyzing the chemical shifts of the paramagnetic signals and the relaxation times of the protons located near the active site.[30] The procedure of 3D structure imaging for proteins is presented in Scheme 1.

Due to the presence of the paramagnetic center in the molecule, the spectral characteristics of the nuclei located in the close vicinity of the paramagnetic center differ appreciably from the corresponding characteristics of the nuclei that do not experience the influence of paramagnetism.[20—22] This allows one to distinguish several dozens of signals from the ^{1}H NMR spectrum containing several hundreds to several thousands of

Scheme 1

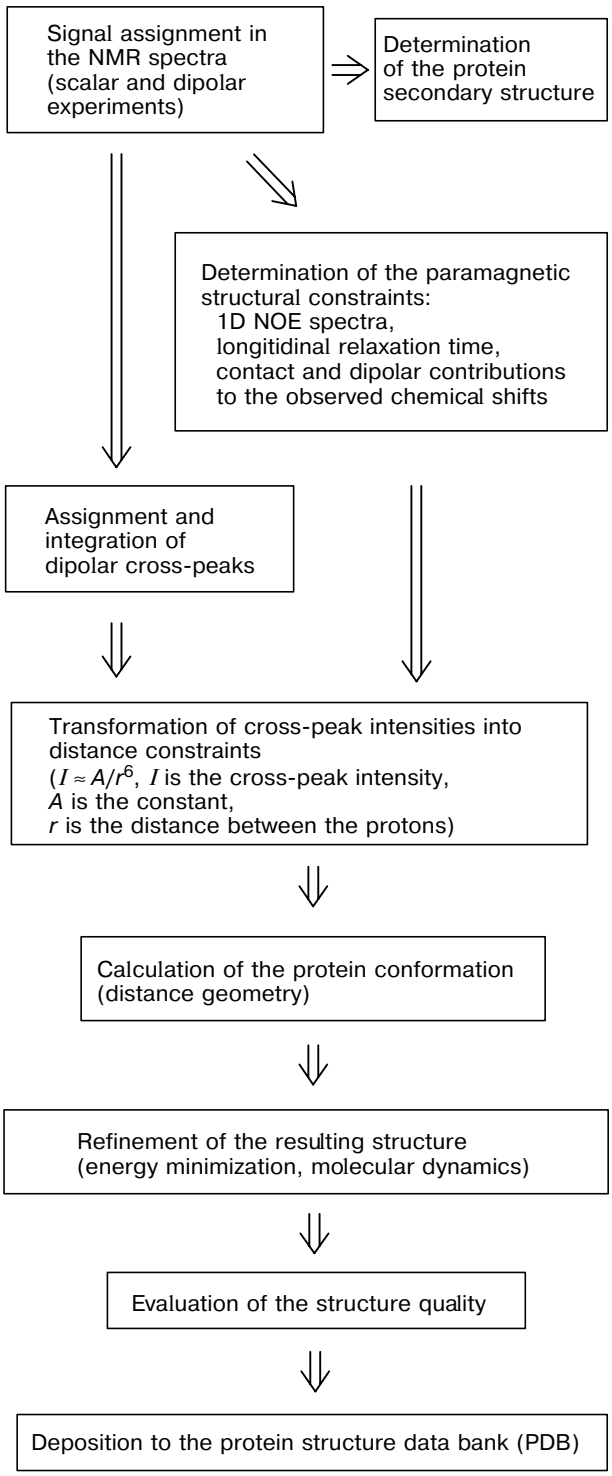

signals and to study only the active site of paramagnetic proteins. This feature of paramagnetic systems is an obvious advantage because it provides the required information on the protein active site without complete investigation of the system.

This review describes the use of the NMR method to determine full three-dimensional structures of iron-sulfur and copper-containing proteins in solution and to study their active sites. This work does not claim to be a thorough enumeration or mentioning of all proteins belonging to these classes and studied by NMR. The purpose of the review is to acquaint the reader with the main achievements and modern approaches to the structural studies of paramagnetic metalloproteins in solution using nuclear magnetic resonance.

Iron-sulfur proteins

Iron sulfur proteins represent a large group of iron-containing nonheme proteins. These proteins contain polymetallic centers (iron-sulfur clusters) in which the iron ions have a tetrahedral coordination geometry and are linked to each other by bridging sulfide ions.[55—59] The iron-sulfur clusters are usually connected to the protein backbone by cysteine residues. However, in some cases, one or several iron ions in the cluster are coordinated by nitrogen of the histidine residue (Risky proteins)[60,61] or by oxygen ligands (aconitase,[62,63] some types of ferredoxins[64—66]). Iron-sulfur clusters differ in the number of iron and sulfur ions and in the structure. The proteins containing one iron ion coordinated to four cysteine residues can also be assigned to this class because they represent the reference point for polymetallic systems.

The tetrahedral or pseudo-tetrahedral environment of Fe^{II} and Fe^{III} ions determines their high-spin state (S = 2, 5/2). The main types of iron-sulfur clusters found in proteins are shown in Fig. 1. The structures of these centers have been established by X-ray diffraction analysis.[67—83] The oxidation states of iron in the most frequently encountered types of iron-sulfur clusters are listed in Table 2. Some iron-sulfur proteins can contain several clusters. Apart from the clusters shown in Fig. 1, clusters with more complicated structures also exist. The [6Fe—6S] clusters have been detected by Mössbauer and ESR spectroscopy.[66,84,85]

Iron-sulfur proteins and enzymes are involved in important biological processes (photosynthesis, respiration, isomerization, *etc.*).[55,58,86] However, the most common function of iron-sulfur proteins is electron trans-

Table 2. Oxidation states of iron ions in the most frequently encountered types of iron-sulfur clusters found in proteins

Cluster types	Protein	Form	
		oxidized	reduced
Fe	Rubredoxin	Fe^{III}	Fe^{II}
Fe_2S_2	Ferredoxin	$2Fe^{III}$	$1Fe^{III} + 1Fe^{II}$
Fe_3S_4	Ferredoxin	$3Fe^{III}$	$2Fe^{III} + 1Fe^{II}$
Fe_4S_4	Ferredoxin	$2Fe^{III} + 2Fe^{II}$	$1Fe^{III} + 3Fe^{II}$
Fe_4S_4	HiPIP	$3Fe^{III} + 1Fe^{II}$	$2Fe^{III} + 2Fe^{II}$

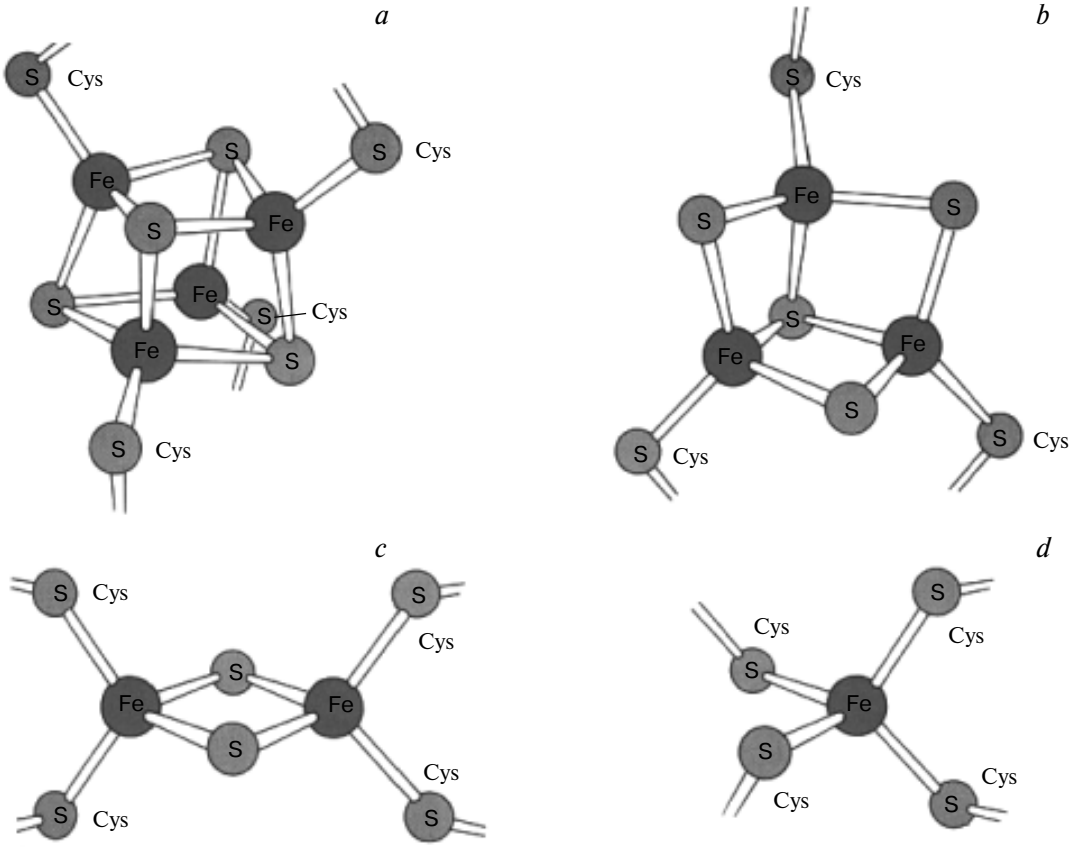

Fig. 1. Structure of iron-sulfur clusters encountered in biological systems. (*a*) 4Fe cluster, ferredoxin, HiPIP, $q = -3, -2, -1$; (*b*) 3Fe cluster, aconitase, $q = -3, -2$; (*c*) 2Fe cluster, ferredoxin, $q = -3, -2$; (*d*) 1Fe cluster, rubredoxin, $q = -2, -1$.

fer.[55,58,86] These systems attracted considerable interest in researchers. Apart from X-ray diffraction analysis, iron-sulfur proteins have also been characterized by various physicochemical methods.[55] Extensive use of NMR spectroscopy for structural and physicochemical investigations has long been impossible. Substantial progress in this field has been made in recent years.[46] The use of specific techniques for the detection of NMR signals of rapidly relaxing ions permitted the first determination of the structure of a paramagnetic protein in solution for the so-called high potential iron-sulfur protein (HiPIP).[87—89]

Mononuclear iron-sulfur proteins

This class of proteins includes rubredoxins,[90,91] desulforedoxins,[92,93] desulfoferredoxins,[94] and rubreritrins.[95] They have relatively low molecular weights (6—12 kDa), and their redox potentials vary from approximately +200 to −150 mV *vs.* the standard hydrogen electrode.[96] The iron ion in these proteins is coordinated to four cysteine residues and has a tetrahedral coordination geometry.[90] In the oxidized state, proteins contain a high-spin Fe^{III} ion, while the reduced form contains a high-spin Fe^{II} ion. The substantial time of electron relaxation of the oxidized iron ion ($\tau_e \sim 10^{-9}$ s) is the reason for considerable broadening of the signals that correspond to protons located near the paramagnetic center.[97,98] Therefore, the signals of the methylene protons of cysteine have not been detected at all in the ^{1}H NMR spectra of the oxidized form. A decrease in the electron relaxation time of the reduced iron ion (Table 1) induces narrowing down of the NMR signals. Indeed, the ^{1}H NMR spectra of the reduced forms of rubredoxins isolated from various sources[98—100] were found to exhibit a number of signals pointing to the presence of paramagnetism. Due to the large linewidths (up to 4500 Hz), the nuclear Overhauser effect (NOE) cannot be observed for these signals; this hampers assignment of these signals to protons for this class of proteins.

This problem can be solved to some extent by deuteration of proteins. The deuterium signals are much narrower than the proton signals because the gyromagnetic constant of deuterium is smaller than that of hydrogen.[21] Thus, it becomes possible to use NMR spectroscopy to characterize rubredoxin derivatives (*Clostridium pasteurianum*) in which all the cysteine residues have been selectively deuterated in the α,β-positions.[101,102] This made it possible to detect and assign the aliphatic signals of all the cysteine residues in the ^{2}H NMR spectrum of rubredoxin in both oxidized

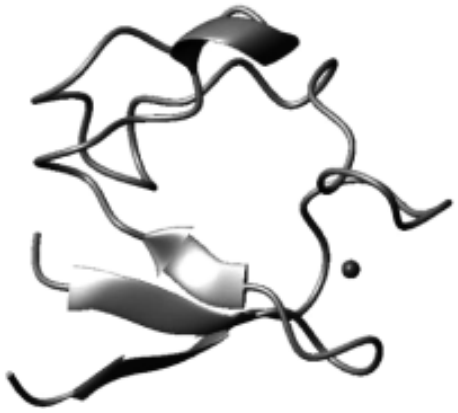

Fig. 2. Three-dimensional structure of the reduced rubredoxin from *Clostridium pasteurianum* in solution with elements of the protein secondary structure.

and reduced forms. As expected, the signals of cysteines are much broadened and located outside the diamagnetic area. In the case of oxidized rubredoxin, the chemical shift of the methylene signals for the cysteine varies from 300 to 900 ppm. The studies performed provided information on the unpaired electron density distribution over the rubredoxin active site.

In addition to assignment of paramagnetic signals, NMR spectroscopy has also been used to determine the structures of proteins of this class. The three-dimensional structure in solution of the reduced form of rubredoxin from *Cl. Pasteurianum* has been determined.[100] The protein structure was calculated taking into account both the standard distance constraints (NOESY spectra) and 36 paramagnetic distance constraints for the metal ions and protons of the surrounding amino acids. These constraints were determined from analysis of the proton longitudinal relaxation time. This gave a family of 20 structures with root-mean-square deviations (RMSD) of 0.58 and 1.03 Å for the backbone and side-chain atoms, respectively. The main skeleton of the mean structure of this family with elements of the protein secondary structure is presented in Fig. 2.

Ferredoxins

A large number of ferredoxins have now been isolated from various organisms and characterized.[75] Apart from differences in the primary structures, these proteins also differ in the structure of the iron-sulfur clusters located in their active sites. In terms of the cluster type, ferredoxins are subdivided into several groups: Fe_2S_2, Fe_3S_4, Fe_4S_4, Fe_7S_8 (contain Fe_3S_4 and Fe_4S_4 clusters), and Fe_8S_8 (contains two Fe_4S_4 clusters). The oxidation states of iron ions in various clusters are listed in Table 2. The redox potential of ferredoxins varies from 0 to −650 mV;[103,104] the molecular weight ranges from 6 to 20 kDa.[75]

As noted previously,[22,42] the interaction between metal ions within the polymetallic center results in an increase in the rate of electron relaxation of metal ions and thus markedly narrows down the signals from the nuclei of the ligands coordinated to the paramagnetic center. However, in the case of oxidized Fe_2S_2-ferredoxin, strong antiferromagnetic interaction between identical Fe^{III} ions does not induce a significant decrease in the electron relaxation time.[105,106] Therefore, the ^1H NMR spectra of the oxidized form of Fe_2S_2-ferredoxins exhibit highly broadened (~2000 Hz) overlapped signals in the low-field region. Such ^1H NMR spectra have been recorded for a number of oxidized Fe_2S_2-ferredoxins.[106—114] Since no data on signal assignment for oxidized ferredoxins of this type are available, neither structural nor electronic information on the protein active site were determined.

In the case of reduced form of Fe_2S_2-ferredoxins, the antiferromagnetic interaction of Fe^{III} ($S = 5/2$) and Fe^{II} ($S = 2$) ions induces a substantial increase in the rate of electron relaxation of metal ions. In the ^1H NMR spectra of reduced ferredoxins of this type, all eight methylene protons of the cysteine residues coordinated to paramagnetic metal ions have been detected.[115] As expected on the basis of theoretical calculations,[116] the signals of the methylene protons of the cysteine residues coordinated to the Fe^{II} ion are located in the region of 45—15 ppm and obey an *anti*-Curie temperature dependence (an increase in the chemical shift of a signal with an increase in temperature).[107,117] The signals of the β-H cysteine residues attached to the Fe^{III} ion exhibit a much greater chemical shift (160—80 ppm) and follow a Curie temperature dependence (a decrease in the chemical shift of the signal with rising the temperature).[115] These differences between the temperature dependences and chemical shifts markedly facilitate the procedure of signal assignment in the spectra of proteins containing polymetallic paramagnetic centers. Analysis of the ^1H NMR spectra and their temperature dependence showed that in this type of ferredoxins, the unpaired electron density is localized on the metal ions.[106,115]

The assignment of the ^1H NMR signals of the cysteine residues was based on analysis of the NOE spectra and structural data for this class of ferredoxins. The presence of signal assignment for the cysteine residues made it possible to find out which of the iron ions (Fe^{II} or Fe^{III}) coordinates each cysteine residue.[108] This sort of structural information cannot be obtained by any other spectral method.

Although determination of the full three-dimensional structures of Fe_2S_2-ferredoxins in solution by NMR is a rather complicated task due to the strong paramagnetism of the polymetallic cofactor, the structures of the oxidized form of the Fe_2S_2-containing ferredoxin from *Synechocystis* sp. PCC 6803[118] or *Synechococcus elongatus*[119,120] cyanobacteria and of the Fe_2S_2-containing ferredoxin from parsley[121] were determined successfully. In the first-mentioned case,[118] the structure

was obtained without constraints for amino acids that experience the influence of the paramagnetic center. This entailed poor resolution of the calculated family and the absence of structural information on amino acids located within a radius of 8 Å from the metal ion. In the case of ferredoxin from *Synechococcus elongatus*,[119] in addition to the 946 distance constraints for the diamagnetic fragment of the protein (derived from analysis of the NOESY spectrum), 241 distance constraints for the 19 amino acids surrounding the cluster were taken into account in structure calculation. The latter constraints were found from analysis of the crystallographic structure of ferredoxin from *Spirulina platensis*. Certainly, the use of X-ray diffraction data obtained for a protein from a different source to calculate the structure in solution does not ensure reliable information about the system under study. In the structure calculation for the ferredoxin from parsley,[121] the paramagnetic distance constraints for the protons located at a distance of up to 5.6 Å from the active site were determined from the NOE spectra and analysis of the longitudinal relaxation time for protons. The use of 2533 distance constraints altogether resulted in a family of structures comprising 18 conformers with a RMSD* of 0.52 and 0.91 Å for the backbone and side-chain atoms, respectively. The structure of the Fe_2S_2-ferredoxin from parsley is the most accurate of all the structures in solution determined by NMR for the given class of proteins.

Apart from this, the structure in solution was determined for oxidized putidoredoxin from *Pseudomonas*, which is a protein containing the Fe_2S_2 cluster in the active site.[122,123] In this case, the paramagnetic broadening of the NMR signals for protons located within a sphere of an iron-sulfur cluster with a radius of ~8 Å precluded determination of experimentally justified structural constraints for this part of the protein to be used in structure calculations.

Fe_3S_4-ferredoxins have been isolated from various bacterial sources.[64,75,124–127] The total spin of the $Fe_3S_4^+$-cluster equals 1/2; it is due to the antiferromagnetic interaction of the three Fe^{III} ions in the oxidized form of the protein.[128,129] The ^1H NMR spectra of the oxidized forms of these proteins contain four signals that experience paramagnetic broadening and are markedly shifted downfield.[130–133] Two of them obey the Curie temperature dependence and display reciprocal dipolar interaction in the NOE spectra. This indicates that the signals belong to the β-H protons of the same cysteine residue coordinated to one iron atom of the cofactor. The other two signals follow an *anti*-Curie-temperature dependence, do not exhibit dipole—dipole interaction (no cross-peaks in the NOE spectra), and correspond to the β-H protons of the other two cysteine residues. The signals that experience a paramagnetic shift were assigned from the analysis of the 1D NOE spectra and the crystallographic data for Fe_3S_4-ferredoxins.[132–134]

* Root-mean-square deviation.

In a Fe_3S_4 cluster, each iron ion interacts with the other two iron ions. The strength of this interaction is described by the J constant (the Heisenberg coupling constant). These three constants can be calculated from the chemical shifts of the methylene protons of the cysteine residues.[135] The observed distribution of signals of the β-H protons of the cysteine residues in the ^1H NMR spectra of the Fe_3S_4-ferredoxins was described by the scheme of symmetric magnetic interaction. According to this scheme, two Fe^{III} ions are equivalent. Their antiferromagnetic coupling constant, J, is greater than the other two coupling constants (see below).[130,131] In other words, the magnetic interaction in a pair of iron ions (ion 1 with ion 2) is stronger than that of ion 1 with ion 3 or ion 2 with ion 3.

The four paramagnetically shifted signals observed in low fields in the ^1H NMR spectrum of the oxidized Fe_3S_4-ferredoxin disappear upon reduction of the protein.[134] This is due to the fact that the paramagnetism of the reduced $Fe_3S_4^0$ cluster is much higher ($S = 2$).

The NMR method was used to determine the 3D structure of the oxidized Fe_3S_4-ferredoxin II from *Desulfovibrio gigas*.[136] The structure was calculated using the distance constraints determined from the two-dimensional NOESY spectra (for the diamagnetic part of the protein) and one-dimensional NOE spectra (for the paramagnetic part of the protein). However, the strong paramagnetism of the $Fe_3S_4^+$ cluster precluded the assignment of signals of all amino acids in the ^1H NMR spectrum of this protein. For amino acids whose signals have not been assigned, data derived from X-ray diffraction analysis of the protein have been used in the structure calculation. The family of structures for the oxidized Fe_3S_4-ferredoxin II from *Desulfovibrio gigas* in solution obtained in this way is shown in Fig. 3.

The active site of the Fe_4S_4-ferredoxins contains a cubic iron-sulfur cluster consisting of four iron ions and

Fig. 3. Family of structures (15 conformers) of the oxidized Fe_3S_4-ferredoxin II from *Desulfovibrio gigas* in solution (elements of the protein secondary structure are shown).

four sulfide ions. This type of iron-sulfur cluster can occur, according to Carter's hypothesis,[137] in three redox states, namely, $Fe_4S_4^+$, $Fe_4S_4^{2+}$, and $Fe_4S_4^{3+}$. In Fe_4S_4-ferredoxins, transition between the $Fe_4S_4^+$ and $Fe_4S_4^{2+}$ states takes place. Two clusters of this type are contained in Fe_8S_8-ferredoxins. The redox potentials of the Fe_4S_4- and Fe_8S_8-ferredoxins vary from −250 to −650 mV.[103,104] The $Fe_4S_4^{2+}/Fe_4S_4^{3+}$ redox transition is observed in high-potential iron-sulfur proteins (HiPIP) (see below). The formalism used to describe the Heisenberg exchange interaction in the Fe_4S_4 clusters is the same for ferredoxins of this type and for high-potential sulfur proteins (for details, see the Section devoted to the latter type of proteins).

Like the ^{1}H NMR spectra of other types of ferredoxins, these spectra of the oxidized Fe_4S_4- and Fe_8S_8-ferredoxins exhibit several signals with paramagnetic broadening located in the low-field region (<20 ppm).[112,138—150] These signals correspond to the aliphatic protons of the ligands. As expected, for the given spin state of the $Fe_4S_4^{2+}$ cluster ($S = 0$),[135] all these signals obey the *anti*-Curie-temperature dependence. The signals due to the β-H and α-H atoms of the cysteine residues were assigned using selective deuteration of these amino acids,[142] 1D NOE spectra, and 2D MCOSY and NOESY* spectra.[140,141,143,144,150,151]

The active site of the reduced Fe_4S_4-ferredoxin contains a $Fe_4S_4^+$ cluster. The basic spin state of the reduced cluster is 1/2.[152,153] The ^{1}H NMR spectrum of the reduced form contains paramagnetically shifted signals at about 65—10 ppm with very short longitudinal and transverse relaxation times. These signals obey both the Curie and *anti*-Curie temperature dependences.[148,154,155]

The partially reduced form of the Fe_8S_8-ferredoxins contains $Fe_4S_4^+$ and $Fe_4S_4^{2+}$ clusters. Apart from the paramagnetically shifted signals corresponding to two different redox forms, the ^{1}H NMR spectra of the semireduced form exhibit signals due to the semireduced form itself.[155] The fact that one ^{1}H NMR spectrum contains signals corresponding to three forms indicates that the equilibrium between them is slow on the NMR time scale. The use of exchange NMR spectroscopy (2D EXSY spectra) provided assignment for the signals of the reduced and semireduced forms. Analysis of the chemical shifts of the β-H protons of the cysteine residue, ^{13}C NMR data,[156] and electrochemical measurements made it possible to determine the potential of each of the two iron-sulfur clusters present in the protein.[155] The data obtained contribute significantly to the study of functional features of proteins of the given class.

The structures of a number of Fe_4S_4- and Fe_8S_8-ferredoxins were determined by NMR spectroscopy. The structures of the oxidized Fe_4S_4-ferredoxins from *Thermotoga maritima*,[157] *Desulfovibrio africanus*,[158] and *Thermococcus litoralis*[151] were obtained taking into account both distance and angle (torsion angles) constraints. The structural constraints for the paramagnetic regions of the proteins were found from one-dimensional NOE spectra, the rates of longitudinal relaxation of protons located near the cluster, and dependences of chemical shifts of the β-H protons of the cysteine residues on the torsion angles χ^2. This is exemplified in Fig. 4, *a*, which shows the structure of the Fe_4S_4-ferredoxin from *Desulfovibrio africanus*.

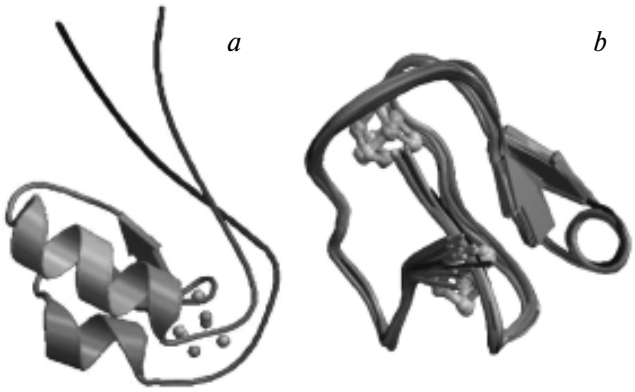

Fig. 4. Three-dimensional structures of the oxidized Fe_4S_4-ferredoxin from *Desulfovibrio africanus* (*a*) and Fe_8S_8-ferredoxin from *Clostridium pasteurianum* (family of 16 conformers) (*b*) in solution with elements of the protein secondary structure.

The calculation of the structures of Fe_8S_8-ferredoxins is markedly complicated by the fact that these proteins are small (they contain altogether 55—60 amino acids); therefore, most of their atoms feel the paramagnetism of the two Fe_4S_4 clusters. Nevertheless, the structure in solution of the oxidized Fe_8S_8-ferredoxin from *Clostridium pasteurianum* was determined.[147] The structure was obtained using for the distance constraints found from the NOESY and NOE spectra, the angle constraints for the torsion angles φ, the distance constraints for the hydrogen bonds, and the angle constraints for the χ^2 torsion angles for the cysteine residues. In total, 456 structural constraints were used to calculate this structure. The RMSD values for the family of structures thus found, which comprises 16 conformers, equal 0.66 and 1.08 Å for the backbone and side-chain atoms, respectively. The family of structures of the Fe_8S_8-ferredoxin from *Clostridium pasteurianum* is shown in Fig. 4, *b*.

The Fe_7S_8-ferredoxins contain the Fe_3S_4 and Fe_4S_4 clusters in their active site. They are characterized by two potentials, *ca.* −250 and *ca.* −550 mV.[159] In the oxidized state, the protein contains the $Fe_3S_4^+$ and $Fe_4S_4^{2+}$ clusters.[86] The total spin of the oxidized protein S is equal to 1/2.[135] During protein reduction, the former cluster [160] is reduced to $Fe_3S_4^0$ with the basic spin state S = 2.[135] The $Fe_4S_4^{2+}$ cluster cannot be oxidized. When an oxidant is added to the protein, oxidative destruction of the tetrameric cluster takes

* COSY is correlation spectroscopy, NOESY is nuclear Overhauser effect spectroscopy, EXSY — exchange spectroscopy.

place.[161,162] The ^{1}H NMR spectra of the oxidized Fe_7S_8-ferredoxins usually exhibit a series of signals characterized by paramagnetic broadening in the low-field region.[149,160,163–167] Study of the temperature dependences of these signals and 1D NOE spectra, and analysis of the ^{1}H NMR spectra of the oxidized/reduced forms of the protein resulted in assignment of each paramagnetically shifted signal and in determination of what cluster is coordinated by each cysteine ligand.[149,166,167] On the basis of the studies performed, it was found that three paramagnetically shifted signals located in the low-field region correspond to the methylene protons of the cysteines linked to the $Fe_3S_4^+$ cluster, two of them being due to the geminal protons of one cysteine residue. The proton signals of the third cysteine ligand have not been detected in the ^{1}H NMR spectra of the Fe_7S_8-ferredoxins until recently. An NMR study of the ferredoxin isolated from *Rhodopsedomonas palustris* and analysis of the available published data allowed the detection and assignment of the β-H signals of all seven ligands of the iron-sulfur clusters.[167] The ^{1}H NMR spectra of the oxidized and reduced forms of the Fe_7S_8-ferredoxin from *R. palustris* are shown in Fig. 5. The spectrum of the oxidized form of the protein contains, apart from the paramagnetically shifted signals located in the low-field region, a paramagnetically broadened signal shifted upfield (signal I). The performed NMR study indicates that this signal corresponds to one methylene proton of the remaining third cysteine ligand of the $Fe_3S_4^+$ cluster. By analyzing the distribution of ^{1}H NMR signals corresponding to the cysteine residues that coordinate the $Fe_3S_4^+$ cluster both in the Fe_3S_4- and in Fe_7S_8-ferredoxins, a correlation has been established between the above-mentioned signal distribution and the primary structures of these proteins.[167]

A NMR study of the Fe_7S_8-ferredoxin isolated from *R. palustris* resulted in the formulation of a new model of magnetic interaction in the $Fe_3S_4^+$ cluster. As noted above, magnetic interaction of the metal ions of the $Fe_3S_4^+$ cluster in Fe_3S_4-ferredoxins can be described by a symmetric scheme ($J_{1,2} \neq J_{1,3} = J_{2,3}$). Due to the presence of two different clusters in the Fe_7S_8-ferredoxin molecule, the $Fe_3S_4^+$ cluster in the Fe_7S_8-proteins is less symmetrical as regards the symmetry of magnetic interactions (*i.e.*, more anisotropic) than the same cluster in the Fe_3S_4-ferredoxins. Based on the signal assignment for the cysteine residues attached to the $Fe_3S_4^+$ cluster performed for the Fe_7S_8-ferredoxin from *R. Palustris*, a new scheme for the interaction within the three-dimensional cluster was proposed. According to this asymmetric scheme, all the coupling constants of the three iron ions are different ($J_{1,2} \neq J_{1,3} \neq J_{2,3}$).[167]

The NMR method was used to determine the three-dimensional structures of the oxidized native Fe_7S_8-ferredoxin from *Bacillus schlegelii*[168] and of the Asp13Cys derivative of this protein.[169] In the latter case, the introduction of an additional cysteine residue into the molecule converts the Fe_7S_8-protein into the Fe_8S_8-ferredoxin. Both structures were calculated taking into account the distance constraints determined from the NOESY and NOE spectra and the angle constraints for the χ^2 torsion angles of the cysteine residues coordinating the iron-sulfur clusters. The latter were found

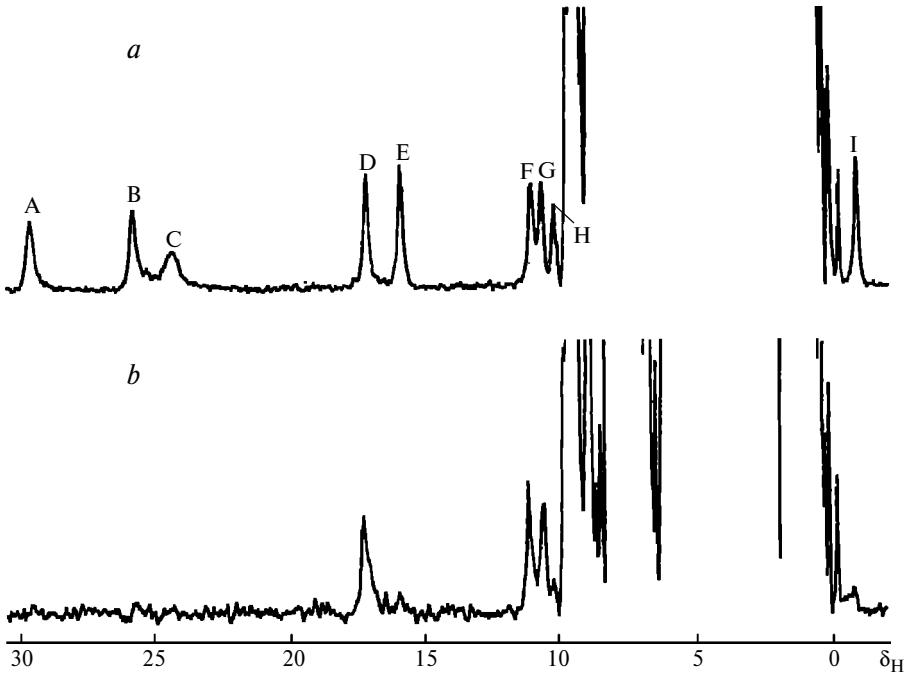

Fig. 5. ^{1}H NMR spectra (500 MHz) of oxidized (*a*) and reduced (*b*) Fe_7S_8-ferredoxin from *Rhodopsedomonas palustris* (298 K, pH 7.0, 50 *mM* phosphate buffer).

Fig. 6. Three-dimensional structure of oxidized Fe_7S_8-ferredoxin from *Bacillus schlegelii* in solution with elements of the protein secondary structure.

from analysis of the angular dependence of the chemical shifts of the proton signals for the cysteine residues. The resulting families of structures consisting of 20 conformers have RMSD of 0.68 and 1.16 Å (native protein) and 0.55 and 0.99 Å (mutant protein) for the backbone and side-chain atoms, respectively. Despite the substantial paramagnetism of these proteins, the use of paramagnetic geometric constraints (distance and angle) provided calculation of these families with a good resolution. The structure of the oxidized native Fe_7S_8-ferredoxin from *Bacillus schlegelii* is presented in Fig. 6.

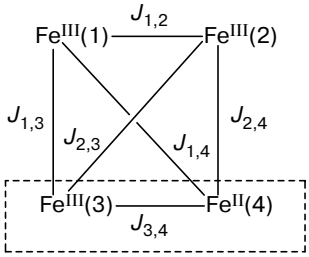

Fig. 7. Scheme of the Heisenberg exchange interaction in the $Fe_4S_4^{3+}$ cluster of the active site of oxidized high-potential iron-sulfur proteins (HiPIP).

High-potential iron-sulfur proteins

High-potential iron-sulfur proteins (HiPIP) contain the 4Fe—4S tetramer cluster in the active site [170] and possess high redox potentials. The $E_{1/2}$ values for these proteins vary from +50 to +350 mV,[56,170,171] while the molecular mass varies from 8 to 10 kDa.[56,170]

As in the case of Fe_4S_4-ferredoxins, the metal ions in the iron-sulfur cluster undergo the Heisenberg exchange interaction, which can be represented (from Mössbauer spectroscopy[172,173]) as interaction of two pairs of metal ions. In the case of the reduced form of HiPIP, the two pairs have fractional oxidation numbers (+2.5) (each pair contains Fe^{II} and Fe^{III}) and are identical. The oxidized form of the cluster is a combination of two pairs of ions; one of them has a fractional oxidation number, while the other comprises two oxidized iron ions. The metal ions in each pair experience ferromagnetic interaction with each other. The scheme of the exchange interaction in the $Fe_4S_4^{3+}$ cluster is presented in Fig. 7. The basic spin states for reduced

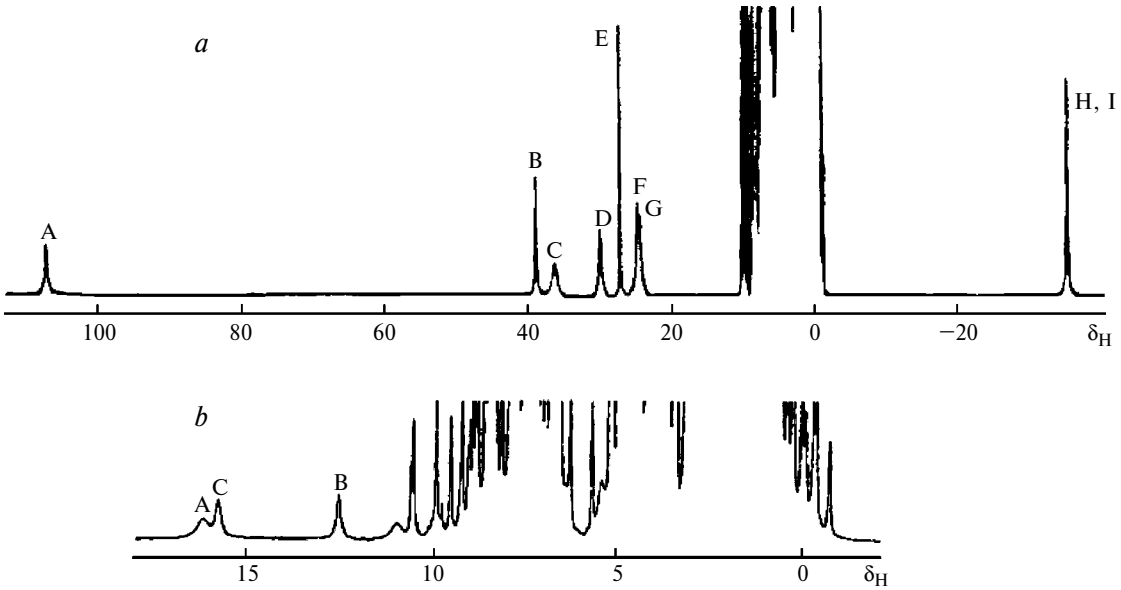

Fig. 8. ^1H NMR spectra (600 MHz) of the oxidized (*a*) and reduced (*b*) HiPIP protein from *Chromatium vinosum* (298 K, pH 7.0, 50 *mM* phosphate buffer).

and oxidized HiPIP are 0 and 1/2, respectively.[135,174,175] These spin states result from antiferromagnetic interaction of the two above-mentioned pairs of iron ions. Thus, the reduced form of the protein should be diamagnetic. However, due to the close proximity of the basic diamagnetic level to the overlying excited paramagnetic energy levels, these levels are partially occupied at room temperature.[176] Thus, the reduced protein is paramagnetic, although its total spin is equal to zero. Indeed, the ^{1}H NMR spectrum of the reduced form is a typical spectrum of a paramagnetic protein. The ^{1}H NMR spectrum of the oxidized and reduced HiPIP isolated from *Chr. vinosum* are presented in Fig. 8. The spectra of both forms of the protein contain signals located outside the diamagnetic region (10—0 ppm), indicating paramagnetism of both forms.

All the signals exhibiting a downfield paramagnetic shift in the ^{1}H NMR spectrum of the reduced HiPIP correspond to the β-H protons of the cysteine residues.[46] All signals obey the *anti*-Curie temperature dependence. The methylene signals of cysteines were assigned using the NOE, NOESY, and COSY spectra and published[46] structural data for these proteins. The one-dimensional NOE spectra recorded with saturation of the paramagnetically shifted signals in the reduced HiPIP from *Chr. vinosum* are shown in Fig. 9 together with signal assignment.

According to theoretical calculations carried out for the oxidized HiPIP,[106,177] the ^{1}H NMR signals for the methylene protons of the cysteine residues coordinated to the mixed-valance pair are expected to shift downfield and to obey the Curie temperature dependence. In contrast, the proton signals of the cysteine residues linked to the oxidized pair of iron ions should experience upfield shift and obey the *pseudo*-Curie-temperature dependence (essential decrease in the chemical shift of the paramagnetically shifted signals following a decrease in temperature (negative chemical shifts)). This theoretical model has been confirmed only partly by experiments. When comparing the distribution, the assignment, and the temperature dependences of the ^{1}H NMR signals of the oxidized HiPIP proteins, one should note that these characteristics depend on the source of the protein. Table 3 summarizes the assignment and the chemical shifts for all the paramagnetically shifted signals of the oxidized HiPIP isolated from various sources. It can be seen from the Table that, in the case of the protein from *Ectothiorhodospira halophila* II,[178a] the methylene signals due to two cysteine residues (Cys I and Cys IV) are shifted upfield and obey a *pseudo*-Curie-temperature dependence, whereas similar signals for Cys II and Cys III are markedly shifted downfield and exhibit the Curie temperature dependence. In the ^{1}H NMR spectra of the other proteins presented in Table 3, only the methylene signals for Cys I are shifted upfield, whereas the signals for Cys IV are located in low field and follow the *anti*-Curie-temperature dependence. As an example, Fig. 10 presents the temperature

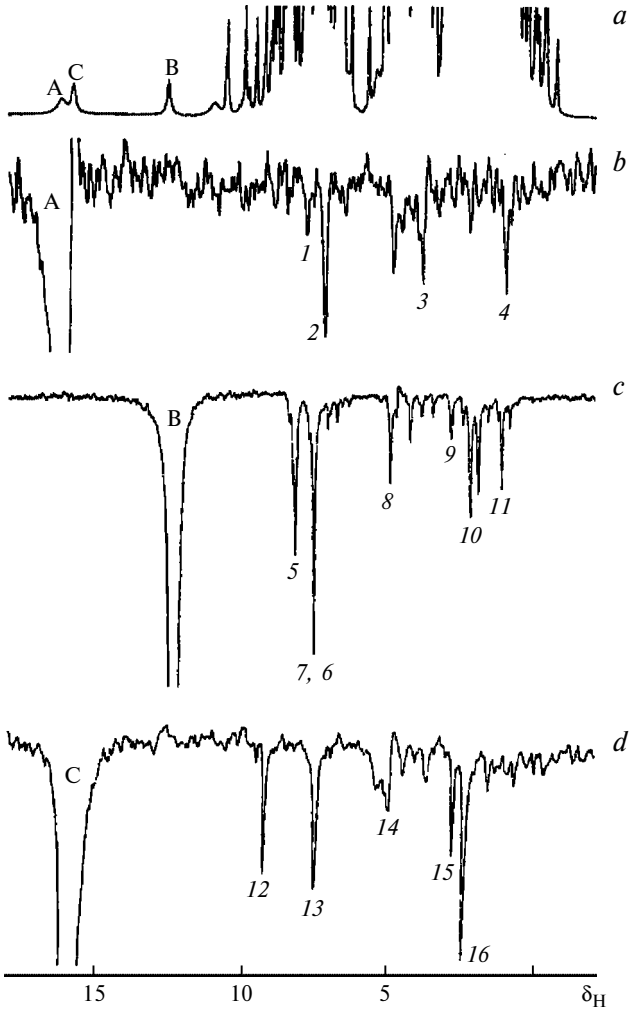

Fig. 9. ^{1}H NMR spectra (600 MHz) of the reduced HiPIP protein from *Chromatium vinosum*: (*a*) reference 1D spectrum, (*b—d*) NOE spectra obtained upon saturation of paramagnetic signals: (*b*) saturation of the β-H(2) signal of the Cys43 residue, (*c*) saturation of the β-H(1) signal of the Cys77 residue, (*d*) saturation of the β-H(2) signal of the Cys63 residue. Assignment of the observed NOE signals: (*1*) NH Ala44, (*2*) β-H(1) Cys43, (*3*) α-H Val73, (*4*) δ-Me Ile71, (*5*) α-H Cys77, (*6*) NH Ala78, (*7*) β-H(2) Cys77, (*8*) α-H Tyr19, (*9*) β-H Tyr19, (*10*) β-H Leu17, (*11*) δ-Me Leu17, (*12*) NH Cys63, (*13*) δ-H Phe66, (*14*) NH Phe66, (*15*) β-H(2) Phe66, (*16*) β-H(1) Phe66. A, B, C are paramagnetic signals. The spectra were recorded at 290 K, pH 5.1, in a 50 *mM* phosphate buffer (D_2O).

dependences of all paramagnetic signals located beyond the diamagnetic area in the ^{1}H NMR spectrum of the oxidized HiPIP protein from *Chr. vinosum*.[179] These signals were assigned both using the NOE spectra[180] and by observing the exchange interactions with the reduced form of the protein in the EXSY spectra.[176]

This difference between the ^{1}H NMR spectra of the oxidized forms of HiPIP and the deviation from the theoretical model observed for most proteins is due to

Table 3. Chemical shifts of paramagnetically shifted signals of the cysteine residues in the ^{1}H NMR spectra of oxidized HiPIP from various sources at 300 K

Source	Cys I			Cys II			Cys III			Cys IV			
	Cys	δ		Cys	δ		Cys	δ		Cys	δ		
		β-H(1)	β-H(2)		β-H(1)	β-H(2)		β-H(1)	β-H(2)		β-H(1)	β-H(2)	α-H
E. halophila II[178a]	39	−22.7	−17.2	42	47.2	56.7	55	47.9	92.5	71	−14.2	−8.7	—
R. globiformis[178b]	21	−32.5	−37.7	24	29.2	32.6	33	45.6	108.2	46	—	13.5	18.2
E. vacuolata II[181]	34	−13.9	−24.7	37	22.4	23.7	51	31.9	101.5	65	22.9	29.5	25.1
Chr. vinosum[180]	43	−31.2	−33.0	46	26.4	25.9	63	35.3	105.8	77	37.6	28.9	26.8
R. gelatinosus[178c]	36	−30.9	−24.8	39	11.8	12.9	53	45.1	95.8	67	31.9	39.5	28.4
Rf. fermentants[178d]	38	−33.9	−29.8	41	13.9	14.6	54	46.7	96.9	68	35.3	41.8	—

the existence of an equilibrium between two forms of the $Fe_4S_4^{3+}$ cluster differing in the distribution of the oxidation states of iron ions.[181] The two tetrametic $Fe_4S_4^{3+}$ clusters that differ in the position of the Fe^{3+} and $Fe^{2.5+}$ ions (one of the ions from each the oxidized pair and the mixed-valence pair, respectively) and occur in equilibrium are shown in Fig. 11. Since the ^{1}H NMR spectrum exhibits two signals for the β-H protons in the cysteine residue, this equilibrium is fast on the NMR time scale (in the case of slow process, the methylene protons of the cysteine residues would give rise to four signals).[181] According to this scheme, in all the HiPIP studied, the two signals shifted downfield (signals A and C in Fig. 8, *a*) correspond to the methylene protons of the Cys III residue linked to $Fe^{2.5+}$, while the two signals shifted upfield (Fig. 8, *a*, signals H and I) belong to the Cys I residue coordinated to Fe^{3+}. The positions of the methylene signals of the other two cysteine residues in the ^{1}H NMR spectrum depend on the position of the equilibrium. In the case of HiPIP from *E. halophila* II,[17,178a] the equilibrium is entirely shifted to the left (Fig. 11); thus, the solution contains 100% of form A. In this case, the ^{1}H NMR spectrum entirely corresponds to the theoretical model.[106,177] For proteins from other sources, both forms always occur in solution. Thus in the case of HiPIP from *Chr. vinosum*, a solution was found to contain 20% form A and 80% form B.[17,179,180] The hypothesis of the existence of an equilibrium between two forms of the $Fe_4S_4^{3+}$ cluster is also confirmed by the observed deviations from linearity of the temperature dependences for paramagnetic signals in some oxidized HiPIP [181,182] and by the results of ^{1}H NMR study of the Cys77Ser derivative of HiPIP from *Chr. vinosum*.[179]

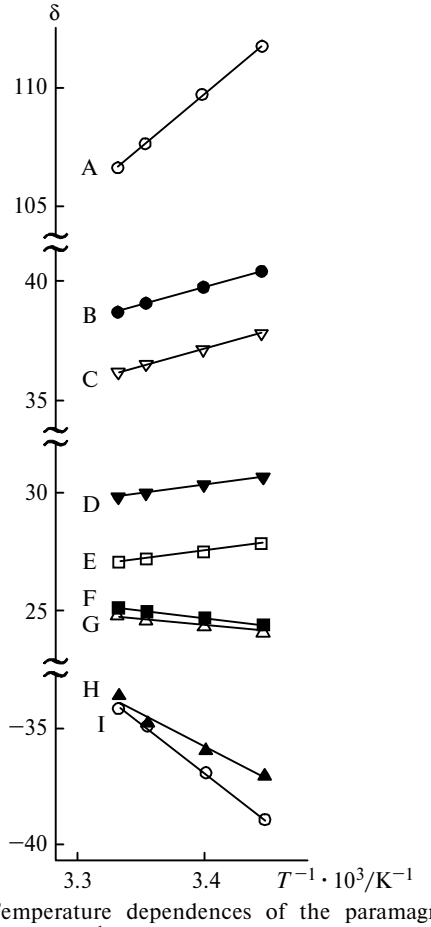

Fig. 10. Temperature dependences of the paramagnetically shifted signals in the ^{1}H NMR spectrum of the oxidized HiPIP protein from *Chromatium vinosum*. The letter designations correspond to the signals in Fig. 8, *a*.

The existence of an equilibrium between two forms of the cluster can also be considered from the standpoint of redox micropotentials of each of the iron ions constituting the cubic iron-sulfur cluster. In the $Fe_4S_4^{3+}$ cluster, one of the four iron ions would always have a

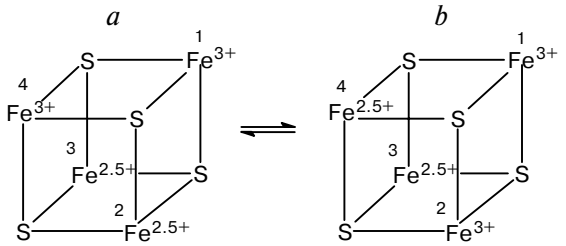

Fig. 11. Scheme of the equilibrium between two $Fe_4S_4^{3+}$ clusters in the active site of the oxidized high-potential iron-sulfur proteins.

charge of +3 (Fig. 11, Fe^{3+}(1)), and the charge of one ion is always +2.5 (Fig. 11, $Fe^{2.5+}$(3)). The redox state of the two remaining iron ions (Fig. 11, Fe(2) and Fe(4) ions) depends on the position of the equilibrium. However, one of these ions would always be in the Fe^{3+} state, while the other would be in the $Fe^{2.5+}$ state. The oxidation state of these ions can be determined from the chemical shifts of the proton signals of the ligands and from the temperature dependence of the signals. Analysis of the ^{1}H NMR spectra of the oxidized HiPIP from various sources made it possible to determine the relative micropotentials of each metal ion within the oxidized tetrameric cluster: Fe(3) > Fe(4) ≈ Fe(2) > Fe(1).[179]

As noted above, the ^{1}H NMR spectra of the oxidized HiPIP can be interpreted using exchange spectroscopy (one-dimensional saturation transfer experiments and two-dimensional EXSY spectra) taking into advantage the ^{1}H NMR signal assignment for the reduced form of the protein.[176,177,183] The fact that signals of both reduced and oxidized forms can be found in one ^{1}H NMR spectrum means that the intramolecular electron exchange between two redox forms is slow on the NMR time scale. Thus the rate constants for the intramolecular transfer of an electron between the reduced and oxidized forms were estimated for a series of high-potential iron-sulfur proteins. The change in the signal intensity, η, upon signal saturation in the saturation transfer spectra is related to the rate constant k' for the observed pseudo-first order exchange process by the following equation:[184]

$$\eta = k'/(R + k'),$$

where R is the rate of the longitudinal relaxation of the proton in the reduced form, k' is the reciprocal lifetime of the reduced form of the protein.

If intramolecular electron exchange follows second-order kinetics, the k' value is related to the second-order rate constant k by the equation

$$k' = k[\mathrm{Ox}],$$

where [Ox] is the concentration of the oxidized form.

The k values for HiPIP from various sources determined by this method vary from 10^3 to 10^6 L mol^{-1} s^{-1}. Differences can be due to several factors, namely, the total charge of the protein, the accessibility of the iron-sulfur cluster to the solvent molecules, and the strength of hydrophobic interactions.[183]

The three-dimensional structures of the reduced and oxidized forms of HiPIP from *Chr. vinosum*[87,88] and *E.halophila II*[89,185] have been determined by NMR spectroscopy. In addition, the structure of the reduced Cys77Ser of the mutant HiPIP from *Chr. vinosum* was calculated.[186] In this review, determination of the structures of paramagnetic proteins and their analysis are considered in detail taking HiPIP from *Chr. vinosum* as an example.

In order to obtain a high-resolution structure, the maximum number of signals should be assigned in the NMR spectrum of the protein under study. The signals in the spectra of oxidized and reduced HiPIP forms from *Chr. vinosum* were assigned using a standard procedure.[15,187,188] By comparative analysis of the two-dimensional TOCSY* and NOESY spectra, the chemical shifts of signals corresponding to 69 amino acids in the spectra of both forms were determined. Analysis of three-dimensional spectra (TOCSY—HMQC**, NOESY—HMQC) allowed the assignment of signals of the NH groups with the same or close chemical shifts. As an example, Fig. 12 presents several F1—F3 (^{1}H—^{1}H) planar cross-sections of the three-dimensional NOESY—HMQC spectrum corresponding to different ^{15}N chemical shifts.[87] The signals in the ^{15}N NMR spectra of both forms of this protein were assigned by analyzing the 3D spectra mentioned above and also the 2D ^{1}H—^{15}N HMQC spectra.

The specific assignment of the protons in the reduced and oxidized forms of the protein carried out by traditional NMR methods used for diamagnetic systems is presented in Fig. 13. For some amino acids, sequential NMR interactions (NH_i—$H_{\alpha i-1}$) have not been identified for the following reasons: the spectral overlap of signals and the absence of sequential interactions in the proline residues. However, the main reason is the close arrangement of some amino acids to the paramagnetic cluster, resulting in broadening of the signals of the corresponding protons and precluding detection of these signals by traditional methods. Their assignment of these signals was based on experimental techniques developed for detection of rapidly relaxing nuclei. These include specially modified TOCSY and NOESY spectra,[37] one-dimensional NOE experiments, which are 1D analogs of the 2D NOESY spectra and are characterized by enhanced sensitivity, NOE—NOESY spectra.[189] Note that 1D NOE spectra can serve as an important source of structural information in investigations of paramagnetic systems because they enable the assignment of the signals of protons located in the close vicinity of the paramagnetic center. Additional structural constraints related to the system paramagnetism can be derived from other NMR experiments.[19,30] Measurement of the longitudinal relaxation times for protons located in the vicinity of the paramagnetic center would make it possible to determine the distance constraints between the protons and the metal ion. Determination of the contribution of the dipolar interaction of the unpaired electron with the nucleus to the observed nuclear chemical shift allows one to calculate the magnetic susceptibility tensor for the given system. This, in turn, provides the distance constraints between the protons and the paramagnetic center of the protein. The angle constraints for the metal ligands can be found from analysis of the chemical shifts of the ligand nuclei. Some of the geometric constraints mentioned above have been

* TOCSY is the total correlation spectroscopy.

** HMQC is heteronuclear multiquantum coherence spectroscopy.

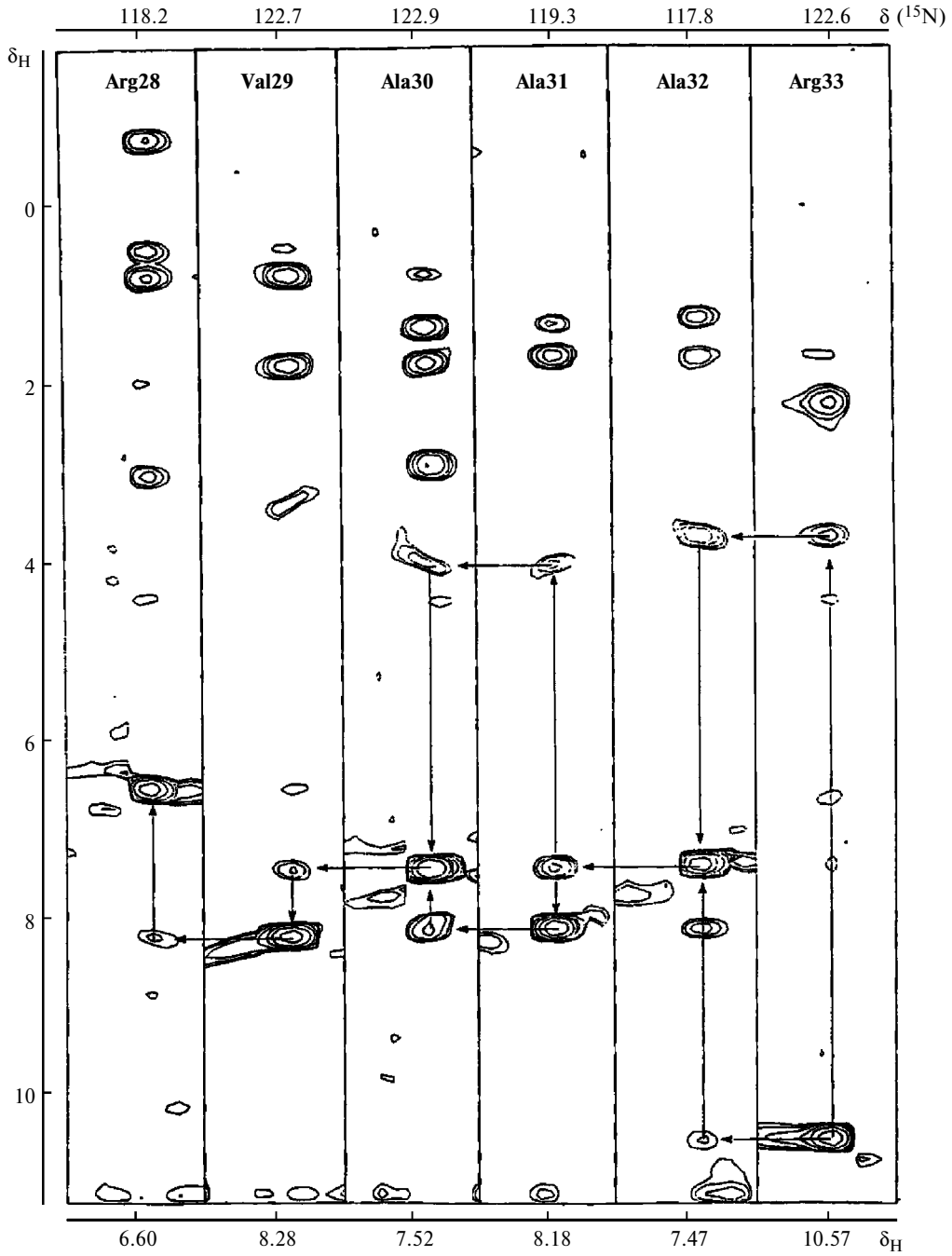

Fig. 12. F1—F3 planar cross-sections of the 3D ^{1}H-^{1}H NOESY—^{1}H-^{15}N HMQC spectrum of the reduced HiPIP from *Chromatium vinosum*. The spectrum was recorded at 300 K, pH 5.1, in a 50 *mM* phosphate buffer. The specific signal assignments for amino acids 28—33 are marked by arrows. The ^{15}N chemical shift for each plane is indicated.

used when calculating the structures of HiPIP from *E. halophila*.[190]

It is noteworthy that, despite the difficulties arising due to the paramagnetism, it proved possible to assign the signals of 85% of the protons in both redox forms and the signals of 90% and 80% of nitrogen atoms in the reduced[87] and oxidized[88] forms of HiPIP from *Chromatium vinosum*, respectively. These results were attained due to the successful combined use of NMR techniques suitable for the detection and subsequent assignment of both diamagnetic and paramagnetic signals.

The structures of the reduced and oxidized forms of the protein were determined using 1461 and 1498 distance constraints, respectively. Analysis of the 1D NOE spectra recorded with saturation of paramagnetically

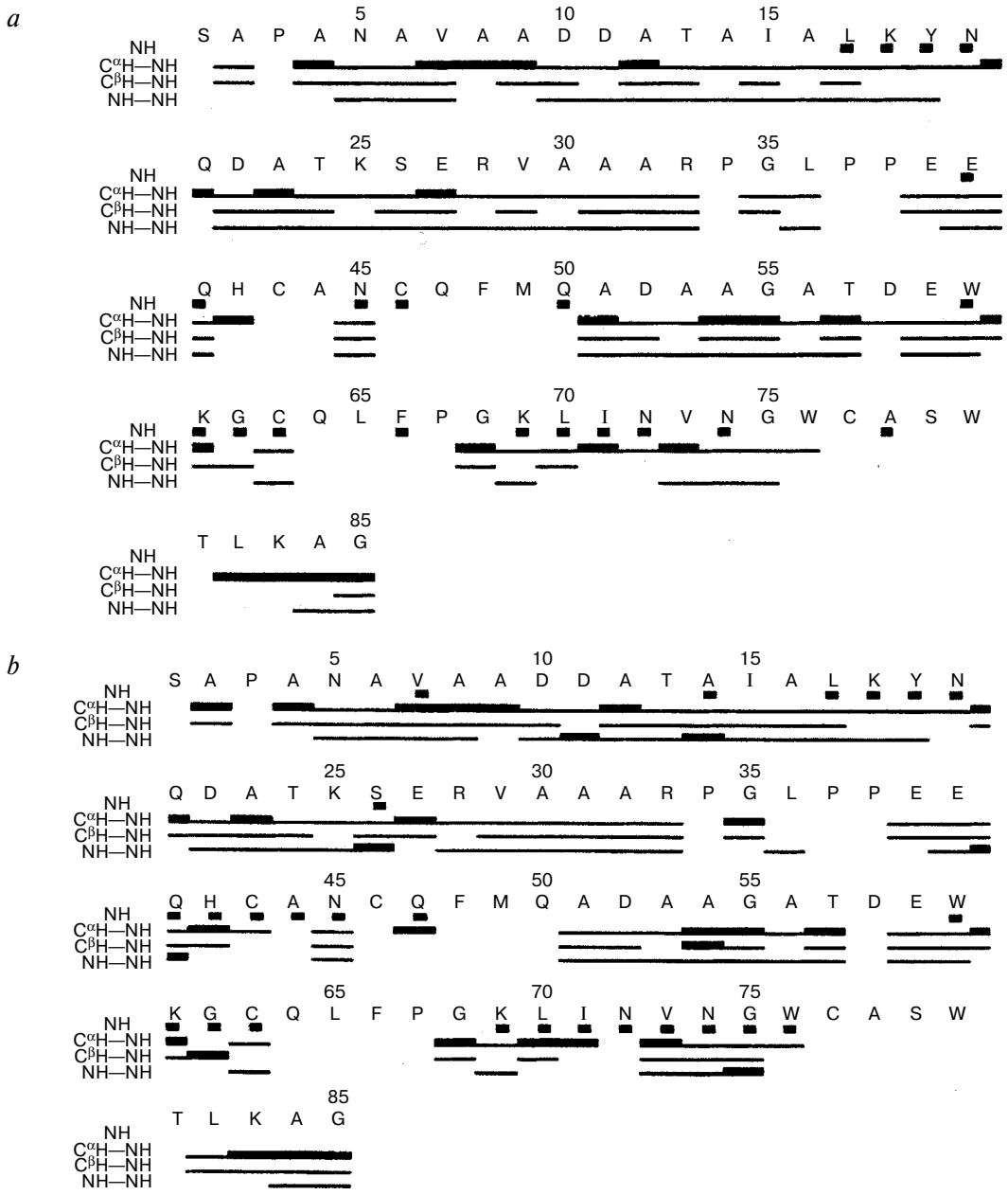

Fig. 13. Schematic sketch of the sequential and medium range NOEs involving the NH, α-H, and β-H protons obtained from standard 2D ^{1}H NMR experiments for the reduced (*a*) and oxidized (*b*) HiPIP protein from *Chromatium vinosum*. The α-H—NH dipole interactions are divided into strong (thick lines) and weak (thin lines) ones. Dark squares correspond to protons that undergo slow exchange with water.

shifted signals corresponding to the β-CH_2 protons of cysteine residues provided 28 and 39 additional distance restrictions for the reduced and oxidized forms, respectively.

Thus, the structures of the reduced and oxidized forms were calculated using, on average, 17.2 and 17.6 distance constraints per amino acid, respectively. These numbers of constraints, which are equal to or greater than those used for diamagnetic proteins having a similar size, ensured high-resolution structures. The structures of oxidized and reduced forms were determined *via* a three-stage calculation procedure including the calculation of the family of distance geometry (DG family),[191] energy minimization (EM family),[192] and, finally, molecular dynamics (MD family).[192] In all calculations, NMR data (distance constraints) were taken into account.

Each of the families thus obtained consisted of 15 structures. The quality of the families was evaluated in terms of the target function (TF) and the RMSD

Table 4. Evaluation of the quality of the resulting structures of the oxidized and reduced HiPIP from *Chromatium vinosum* at each stage of calculation[87,88]

Family	Form	RMSD		Target function		E_{total} /kJ mol^{-1}	Δl /Å	$\Delta\varphi$ /deg
		A_{ch}	A_{sch}	/Å	/kJ mol^{-1}			
DG	Ox	0.67±0.09	1.09±0.10	0.51				
	Red	0.73±0.12	1.13±0.12	0.56				
EM	Ox	0.59±0.09	1.06±0.09		58.46	−5660.0		
	Red	0.69±0.11	1.14±0.11		55.98	−5701.0		
MD	Ox	0.57±0.14	1.08±0.16		70.84	−7214.0		
	Red	0.62±0.12	1.19±0.18		57.07	−7259.0		
MD	Ox_{H_2O}*				75.91	−6609.0	0.007	1.61
	Red_{H_2O}*				44.27	−6648.0	0.007	1.55

Note. RMSD is the root-mean-square deviation for the Ala2-Leu82 amino acids; Δl is the deviation from the ideal bond lengths; $\Delta\varphi$ is the deviation from the ideal bond angles; DG is the distance geometry family; EM is the energy minimization family; MD is the molecular dynamics family; A_{ch} are the backbone atoms, A_{sch} are the side-chain atoms; E_{total} is the total energy.
* With a correction for the solvent—protein interaction.

value. All these parameters characterizing the quality of the families obtained for the oxidized and reduced forms of this protein at each calculation stage are presented in Table 4.

In the further calculation of the molecular dynamics in water, a correction for the solvent—protein interaction was applied. This calculation was carried out for averaged structures of the MD families for the reduced[87] and oxidized[88] forms of the protein. The parameters characterizing the quality of the structures thus obtained (Red_{H_2O} is the structure of the reduced form, Ox_{H_2O} is the structure of the oxidized form) are presented in Table 4. The structure of the reduced form of the protein with elements of the secondary structure is presented in Fig. 14.

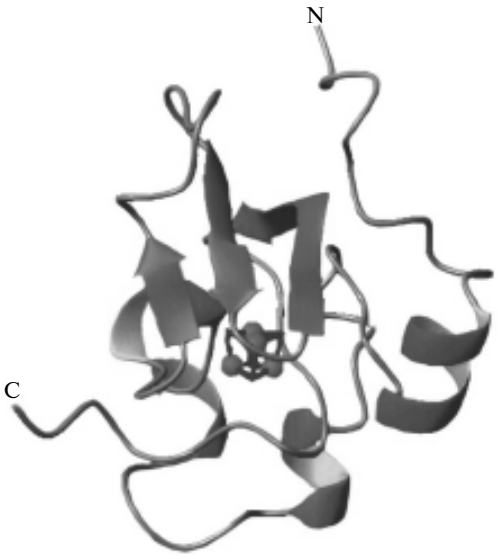

Fig. 14. Three-dimensional structure of the reduced HiPIP protein from *Chromatium vinosum* in solution with elements of the secondary structure of this protein.

Copper-containing proteins

Copper is the second most naturally abundant transition metal after iron.[193] In living organisms, copper exists in two stable oxidation states, Cu^{I} and Cu^{II}. The redox potential of this pair varies over a broad range in different biological processes. The following four types of copper sites can be found in nature:[194]

type 1 that includes mononuclear sites (blue proteins),
type 2 that includes mononuclear catalytic sites,
type 3 that includes binuclear sites, and
Cu_A corresponding to electron transferring binuclear sites.

Other copper sites can be regarded as combinations of the four above-mentioned types. For example, a trinuclear copper site is a combination of the second and third types.[195] The spectra of each type of site have their own characteristic features.[194] In this review, we consider the NMR studies of blue proteins (type 1 sites).

Blue proteins have been found both in bacteria and in plants.[196—199] In addition, type 1 sites are encountered in enzymes containing polynuclear copper sites. In addition to the mononuclear sites (type 1), these enzymes also contain catalytic sites with one or several copper ions.

The redox potential for the first type of sites varies from 180 to 790 mV.[200] This value can be influenced by the nature of the axial ligand, the accessibility of the active site for the solvent, and the charge distribution around the copper ion.[201—204]

Blue proteins possess a number of similar spectral and structural features. A specific feature of the electronic spectra of the oxidized forms of blue proteins is the presence of a ligand—metal charge transfer line ($\pi Cys \rightarrow Cu^{II}$) at about 600 nm.[205—207] It is this interaction that is responsible for the intense blue color typical of the oxidized form. Proteins that belong to this group

have similar secondary and tertiary structures and similar structures of the active site.[196] By analogy with ferredoxins, blue proteins are also called cupredoxins.[196] On the basis of phylogenetic analysis, these proteins can be classified into five subclasses:[208,209] (1) plastocyanin family (plastocyanins, amicyanins, pseudoazurins, halocyanins), (2) aurocyanins, (3) azurin, (4) rusticyanin, (5) phytocyanin family (plantacyanins, stelacyanins, uclacyanins). In most cases, the copper ion in these proteins is coordinated by two histidine residues, one cysteine residue, and one methionine residue, which is the axial ligand.[200] In the case of stelacyanins, the axial methionine is replaced by glutamine.[210] In some cases, the active site of the first-type multinuclear copper enzymes does not contain any axial ligand.[211]

The oxidized paramagnetic form of this class of protein has been little studied by NMR spectroscopy. This is related to the difficulties faced by investigations of paramagnetic systems containing a Cu^{2+} ion by NMR. The reason is the substantialy long electron relaxation time of the copper ion (1—5 ns).[22] As a consequence, the signals from the nuclei located near the copper ion (mainly, the ligand nuclei) are broadened to such an extent that they cannot be detected in the spectrum at all. Therefore, it is still considered that proteins containing an oxidized copper ion can hardly be studied by NMR spectroscopy. Nevertheless, in 1996, the first ^{1}H NMR spectra of blue proteins, amicyanin and azurin were recorded and interpreted using high-resolution NMR technique for detection of rapidly relaxing signal.[212] These spectra were found to reveal a series of paramagnetically shifted signals. These were assigned by virtue of exchange spectroscopy. The ^{1}H NMR spectra for the oxidized forms of a number of other cupredoxins have also been recorded.[213—216] However, until recently, it was impossible to detect all the ^{1}H NMR signals corresponding to the copper-coordinating ligands. This was an obstacle hampering determination of the full electronic structure of active sites. Moreover, the absence of NMR data on the active site in the oxidized form of cupredoxins precludes determination of their three-dimensional structures in solution.

Full assignment of all the ^{1}H NMR signals located outside the diamagnetic region of the spectrum for the oxidized form of proteins was first obtained for the plastocyanin isolated from spinach leaves.[217] The use of a specially developed procedure made it possible to locate the highly broadened signals of the methylene protons of the cysteine residue coordinated to the copper ion. Owing to the ^{1}H NMR investigations performed, the electronic structure for this class of proteins was determined for the first time under conditions close to physiological conditions. Subsequently, the developed procedure was applied for investigations of other blue proteins, namely, plastocyanin from the *Synechocystis sp.* PCC 6803 cyanobacteria,[218] azurin from *Pseudomonas aeruginosa*,[219] and stelacyanin from cucumber.[219] Here we describe in detail the procedure of assignment of the signals that underwent paramagnetic shifts in the spectrum of the oxidized form of blue proteins and determination of the electronic structure of these proteins in relation to the plastocyanin isolated from the *Synechocystis sp.* PCC 6803 cyanobacteria.[218]

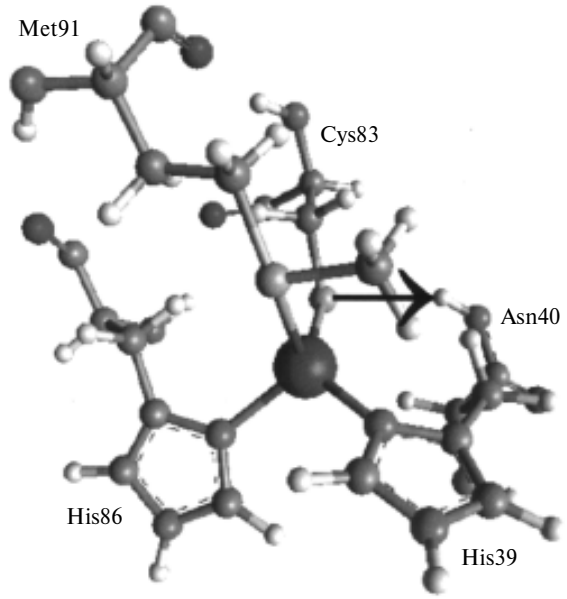

Fig. 15. Structure of the active site of plastocyanin from *Synechocystis sp.* PCC 6803. The arrow marks the hydrogen bond between the amide proton of the Asn40 residue and the γ-S atom of the Cys83 residue.

Plastocyanin is a relatively small (~100 amino acids) protein with a redox potential of about 350—370 mV.[220—222] The active site of this protein has a distorted tetrahedral geometry.[200] The structure of the active site of plastocyanin is shown in Fig. 15. Plastocyanin is a direct electron donor when coupled with the photooxidized chlorophyll dimer (P700) in photo system I.[220—222] After donating an electron, plastocyanin is reduced upon the reaction with cytochrome f incorporated in the b_6f complex. In the oxidized state (Cu^{2+}), this protein exhibits clear-cut paramagnetic properties ($S = 1/2$, d_9), whereas the reduced form is diamagnetic ($S = 0$, d_{10}).

The ^{1}H NMR spectrum of the oxidized plastocyanin from *Synechocystis sp.* PCC 6803 is shown in Fig. 16. As expected, the signals in the spectrum are substantially broadened due to the slow electron relaxation of the Cu^{II} ion.[22] The width of paramagnetic signals varies from 800 to 5000 Hz. The spectra recorded in solutions in H_2O or D_2O (Fig. 16) indicate that, among the paramagnetic signals, three signals (C, F, K) correspond to the NH-group protons of the ligands. This follows from the fact that these signals either cannot be detected in a solution in D_2O or their intensity is markedly lower than that observed in the spectrum recorded in H_2O. All signals were assigned using so-called saturation transfer spectra, which were recorded for a sample

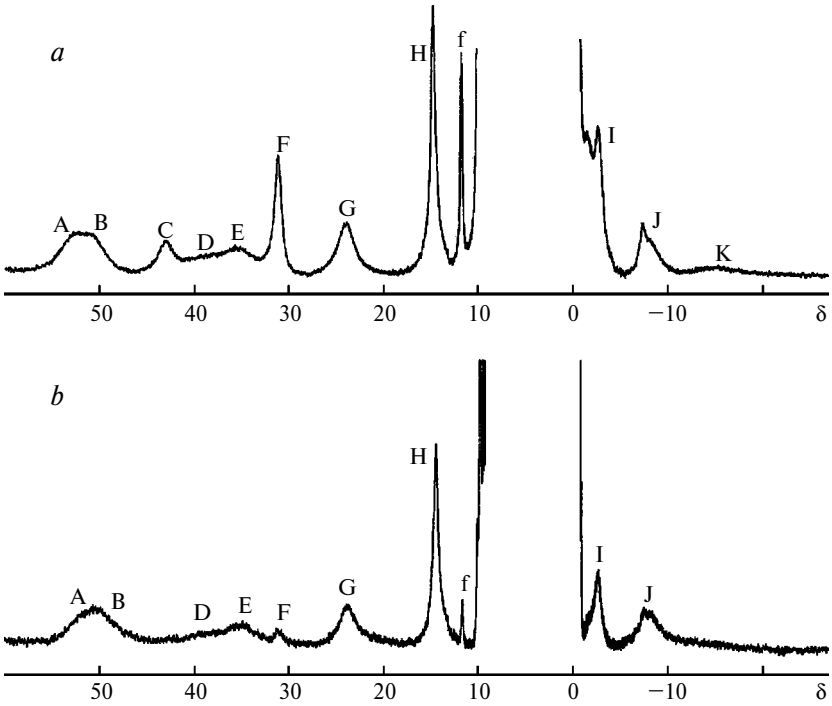

Fig. 16. ^{1}H NMR spectra (800 MHz) of the oxidized plastocyanin from *Synechocystis sp.* PCC 6803 in solutions in H_2O (*a*) and D_2O (*b*) (298 K, pH 5.2, 50 *mM* phosphate buffer).

containing approximately equal amounts of oxidized and reduced forms of the protein. The procedure employed is based on the detection of magnetization transfer between the same proton in two different forms (in the given case, in the reduced and oxidized forms). This type of NMR spectroscopy used to study the dynamic properties of a system is called exchange spectroscopy.[184] This type of approach can be used to monitor the exchange processes in various systems (in the given case, intramolecular electron transfer is investigated) provided that the rate constant of the process meets the following conditions.[21,31,184] On the one hand, the process under study should be sufficiently slow, so that the signals corresponding to two forms can be observed in the same NMR spectrum. Indeed, if the process rate is too high, the spectrum will exhibit one, averaged signal, instead of the two signals corresponding to the two forms. On the other hand, the exchange process should be fast enough to enable NMR monitoring of the magnetization transfer (otherwise, the corresponding signals are not recorded in the saturation transfer spectra). If these conditions are met (the rate constant falls in the favorable range), this type of spectroscopy allows not only the assignment of the NMR signals to the two forms but also determination of the rate constant of the process under study.[184]

The saturation transfer spectra for paramagnetic signals of the protein are presented in Fig. 17. The spectra were obtained with selective homonuclear decoupling. The decoupler is adjusted to the frequency of a definite signal of the oxidized form (signal saturation takes place, resulting in the disappearance of this signal from the ^{1}H NMR spectrum), and then the corresponding signal of the reduced form of the protein was observed in the diamagnetic region of the spectrum. The spectra thus obtained allow one to match paramagnetic signals of the oxidized form of plastocyanin to signals of the reduced form. It should be noted that the signals in the ^{1}H NMR spectrum of the reduced diamagnetic form were assigned using a standard procedure.[223] The spectra shown in Fig. 17 permit the paramagnetic signals of the oxidized form to be readily assigned. Analysis of the NMR data provided an approximate estimate of the rate constant for the electron transfer between the reduced and oxidized plastocyanin. This constant lies in the 10^4—10^7 range (mol s)$^{-1}$. The results obtained are in good agreement with the rate constants for the intramolecular electron transfer determined for other blue proteins.[224]

Study of the active sites of plastocyanins by other spectral methods (ENDOR*, XAS**)[225—227] demonstrated that the larger part of the unpaired electron density of the Cu^{II} ion is delocalized over the cysteine residue coordinated to the copper atom. Theoretical calculations[21] suggest that the signals corresponding to the β-H protons of the Cys83 residue should be very broad and markedly shifted downfield. Indeed, the signals corresponding to the methylene protons of the Cys83 residue have not been detected within the limits

* ENDOR is electron-nuclear double resonance spectroscopy.
** XAS is X-ray absorption spectroscopy.

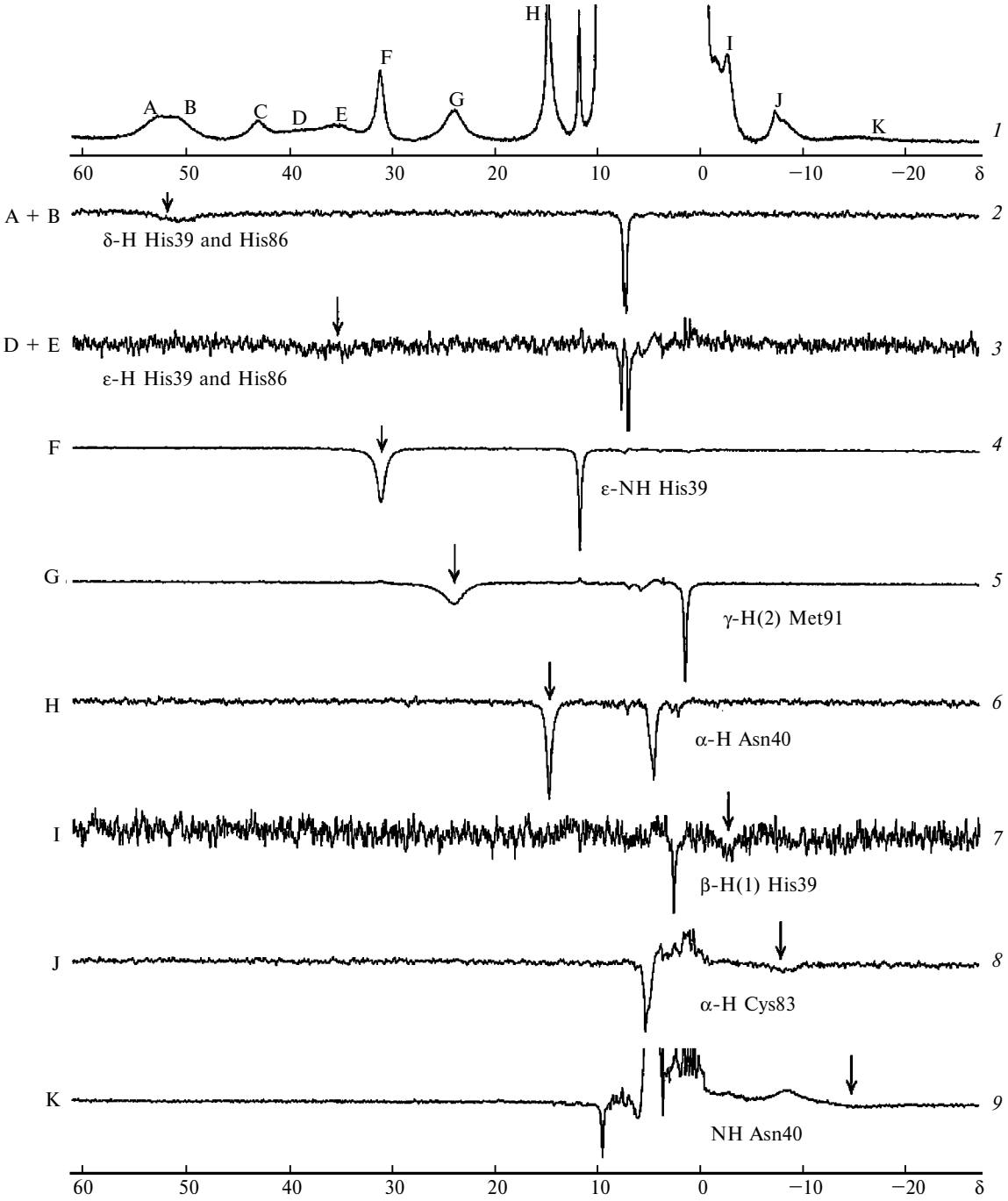

Fig. 17. ^{1}H NMR spectra (800 MHz) of plastocyanin from *Synechocystis sp.* PCC 6803 in an aqueous solution (the sample contains approximately equal amounts of the oxidized and reduced forms of the protein): (*1*) reference 1D spectrum, (*2—9*) saturation transfer spectra. The arrows mark the position of the decoupler during the saturation of signals designated by letters. The spectra were recorded at 298 K, pH 5.2, in a 50 *mM* phosphate buffer.

of the spectral window used to record the spectra shown in Figs. 16, 17. An increase in the spectral window to +1500 to −1500 ppm did not result either in the detection of new signals, apart from those presented in Figs. 16 and 17.

The signals of the β-H protons of the Cys83 residue were identified using a specially developed procedure.[217] According to this procedure, the decoupler is adjusted to a frequency where no signals are observed rather than to a frequency of one particular signal (as was done when recording the spectra presented in Fig. 17). Since the rate constant of the intramolecular exchange by an electron between the two redox forms in this system falls in the favorable range (see above), even slight

saturation of very broad invisible signals of the β-H protons of the cysteine residue makes visible the corresponding signals of the reduced form of the protein in the diamagnetic region of the spectrum. The spectra of magnetization transfer (the regions corresponding to methylene protons) recorded for different positions of the decoupler are presented in Fig. 18. One can see the appearance, growth, decrease, and complete disappearance of two signals at 3.5 and 3.0 ppm in these spectra. The chemical shifts of these signals correspond to the β-H protons of the Cys83 residue of the reduced form.[223] The dependence of the intensity of these signals on the position of the decoupling generator (Fig. 19) allows direct determination of both the chemical shifts of the β-protons of the CH_2 groups in the oxidized form and their linewidth.

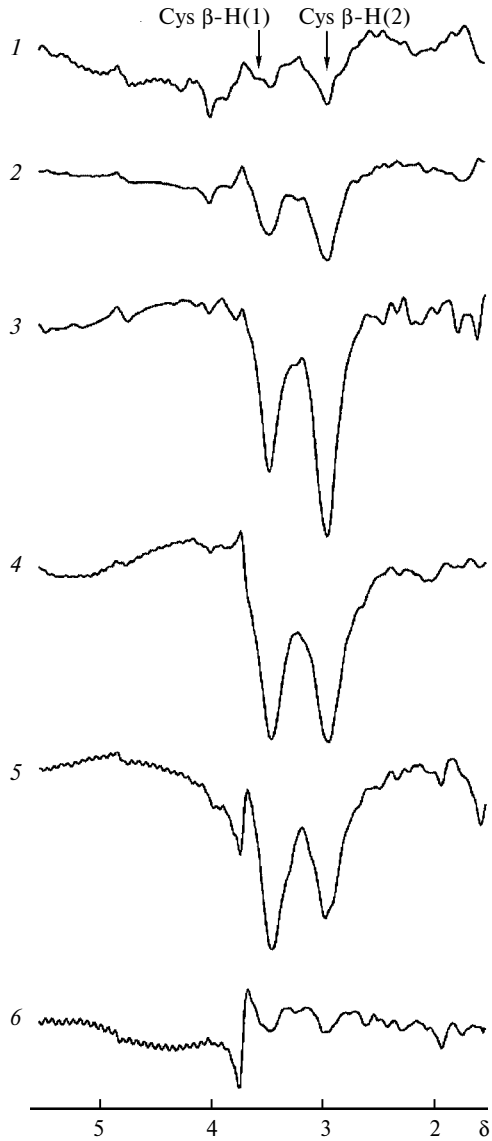

Fig. 18. Saturation transfer ^{1}H NMR spectra (800 MHz) (the region of methylene protons) of plastocyanin from *Synechocystis sp.* PCC 6803 in a D_2O solution. The sample contains approximately equal amounts of the oxidized and reduced forms of the protein. Each spectrum was recorded with adjustment of the decoupler to the suppression of various frequencies: 150 (*1*), 250 (*2*), 450 (*3*), 650 (*4*), 750 (*5*), 1250 ppm (*6*). The positions of the signals of the β-H(1) and β-H(2) protons of the Cys83 residue of the reduced protein is marked by arrows. The spectra were recorded at 298 K, pH 5.2, in a 50 *mM* phosphate buffer.

The chemical shifts of these signals (β-H(1) and β-H(2) of the Cys83 residue) in the oxidized form are 614 and 517 ppm, while their linewidths are 395 and 335 kHz, respectively. The difference between the given parameters and the similar values for diamagnetic signals (chemical shift 0—10 ppm, line width 2—10 Hz) is impressive; it allows one to appreciate the potential of the developed method. Using this method, the β-H signals for the cysteine residue coordinated to the copper atom were located for the first time in the ^{1}H NMR spectra of blue proteins. Certainly, the chemical shifts and the signal widths are maximum among all the analogous data. In addition, the developed method made

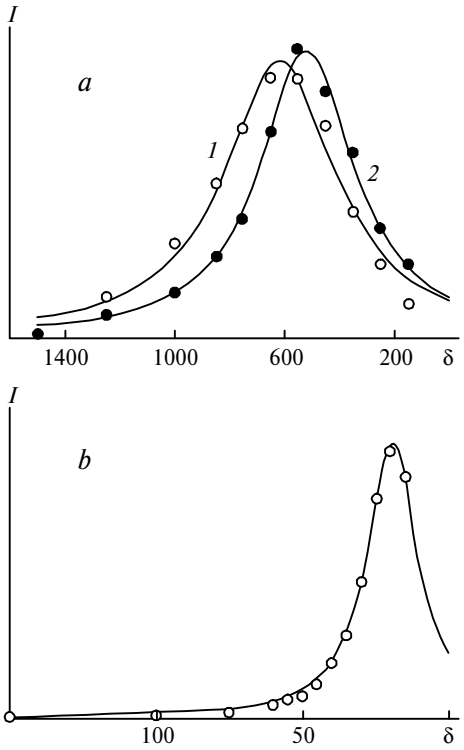

Fig. 19. Intensities of the signals of the β-H(1) (*1*) and β-H(2) (*2*) protons of the Cys83 residue (*a*) and the α-H proton of the His39 residue (*b*) in the ^{1}H NMR spectrum of the oxidized form of plastocyanin from *Synechocystis sp.* PCC 6803 *vs.* position of the decoupler: (*a*) $\Delta\nu$ = 395 kHz (*1*), 335 (*2*), (*b*) $\Delta\nu$ = 16.8 kHz. These signals cannot be detected in a conventional spectrum. The positions and line widths for the given signals were determined using saturation transfer spectra (see the text). These parameters were determined by point construction of a plot in which the intensity of the observed exchange interactions with the reduced form was laid off as a function of the position of decoupler.

it possible to detect the α-H signal of the His39 residue in the ^{1}H NMR spectrum of oxidized plastocyanin (Fig. 19). The chemical shift of this signal and the line width are 19.2 ppm and 16.8 kHz, respectively. Although the width of this signal is smaller than that of the methylene signals in the Cys83 residue, this still prevents direct observation of this signal in conventional ^{1}H NMR spectrum (Fig. 16 and 17).

As has already been noted, the proposed procedure has found use for the detection and subsequent assignment of the highly broadened signals in the ^{1}H NMR spectra of other blue proteins (azurin, stelacyanin).[219] Figure 20 shows the ^{1}H NMR signals of the methylene protons of the cysteine residue coordinated to copper in the oxidized azurin from *Pseudomonas aeruginosa* (*a*),[219] plastocyanin from spinach (*b*),[217] and stelacyanin from cucumber (*c*).[219] These signals were not detected in conventional ^{1}H NMR spectra; their positions and line widths were determined by the above-described procedure. The chemical shifts of these signals and the line

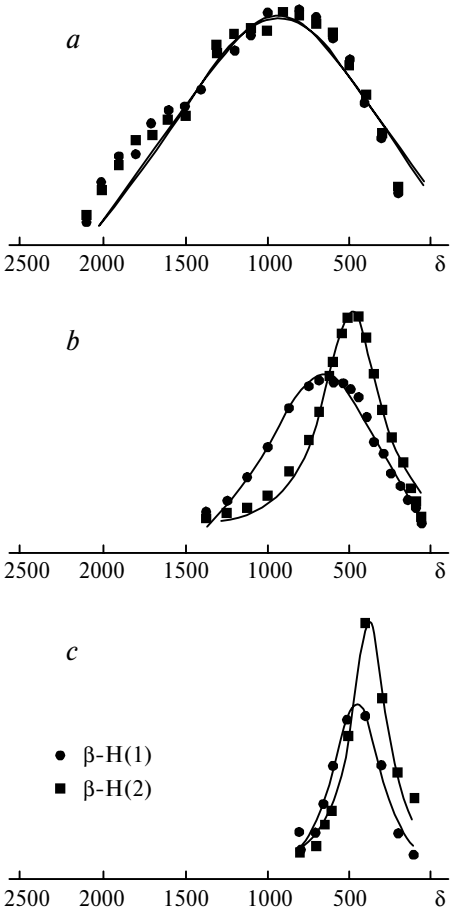

Fig. 20. ^{1}H NMR spectra of the oxidized forms of blue proteins containing the signals of methylene protons, the β-H(1) and β-H(2) protons of cysteine residues: (*a*) azurin from *Pseudomonas aeruginosa*, (*b*) plastocyanin from spinach, (*c*) stelacyanin from cucumber. The positions and widths of the signals were determined using saturation transfer spectra (see the text and the caption to Fig. 19).

widths change substantially on passing from one class of blue proteins to another. The average chemical shifts and line widths of the cysteine methylene signals are 850 and 1.2 for azurin, 600 and 0.45 for plastocyanin, and 400 ppm and 0.25 MHz for stelacyanin. It has been suggested[219] that the differences between the ^{1}H NMR parameters are related to the distance between the copper ion and the axial ligand and to the planarity of the Cu^{II}—$N(His)_2S(Cys)$ group.

The assignments made for paramagnetically shifted ^{1}H NMR signals allowed determining the distribution of the unpaired electron density of the Cu^{II} ion in the active sites of blue proteins. This information was gained from analysis of the observed chemical shifts of signals in the ^{1}H NMR spectrum. The observed chemical shift (δ_{obs}) is known to be the sum of contributions of various types of interaction of the nucleus with electrons, which include[20,21,228]

(1) the contact Fermi shift (δ_{cont}) determined by delocalization of the lone electron density over the nuclei of the amino acid coordinating the metal;[23,24]

(2) pseudo-contact (dipolar) shift (δ_{dip}) determined by the dipolar interaction of the nucleus with lone electrons;[25]

(3) diamagnetic shift (δ_{dm}), *i.e.*, the chemical shift of the nucleus in the diamagnetic system.

In order to determine δ_{con}, it is necessary to know the δ_{dip} and δ_{dm} constituents, apart from the observed chemical shift. The above-described experiments on the magnetization transfer between the oxidized (paramagnetic) and reduced (diamagnetic) forms (Fig. 17) made it possible to determine δ_{dm} for paramagnetic signals. The δ_{dip} value was found from formula (1) using the structure and published data on the *g*-tensor of this protein:[207,229,230]

$$\delta = \frac{\mu_0}{4\pi}\frac{\mu_B^2 S(S+1)}{9kTr^3}(3\cos^2\theta - 1)(g_\parallel^2 - g_\perp^2)10^6, \qquad (1)$$

where μ_0 is the magnetic susceptibility of vacuum, μ_B is the Bohr magneton, k is the Boltzmann constant, S is the total spin of the system, T is absolute temperature, r is the distance between the proton and the copper ion, $g_\parallel$, $g_\perp$ are the directions of the principal axes of the axial *g*-tensor, and θ is the angle between the metal—proton vector and the $g_\parallel$-axis.

Thus, the contribution of δ_{con} was defined as the difference between the observed chemical shift and the dipolar and diamagnetic shifts. The hyperfine structure constant a was determined using Eq. (2)[229,230]

$$\frac{a}{h} = \frac{1}{2\pi}\frac{\delta_{con}\, 3\gamma_N kT}{g_{av}\mu_B S(S+1)}, \qquad (2)$$

where γ_N is the gyromagnetic ratio of the nucleus, δ_{con} is the contribution of the contact interactions to the observed chemical shift, g_{av} is the averaged value of the electronic *g*-factor, and h is the Planck constant.

The hyperfine structure constants can be used to estimate the electron density on each nucleus. The hyperfine structure constants calculated for all protons in the active site of the oxidized plastocyanin from *Synechocystis sp.* PCC 6803 are listed in Table 5.

It can be seen from Table 5 that most of the electron density is delocalized over cysteine coordinated to copper. According to the rough estimate based on the results obtained and the results of ENDOR studies of blue proteins,[225,231] 40% of the unpaired electron density is delocalized over the cysteine residue, 5% is delocalized over each of the histidine residues, and 2% is on the methionine residue. It should be noted that Asn40 that is not coordinated to the copper ion also bears ~5% of the electron density. The amide proton of this amino acid forms a hydrogen bond with the Sγ atom of Cys83 (see Fig. 15). The investigations performed demonstrated that the unpaired electron density of the copper ion is distributed not only over the ligands (His39, Cys83, His86, Met91) but also through the above-mentioned hydrogen bond over Asn40. A similar transfer of the unpaired electron density through a hydrogen bond was found for azurin from *Pseudomonas aeruginosa*,[219] plastocyanin from spinach,[217] and stelacyanin from cucumber.[219] The rest of the unpaired electron density (~40%) remains on the Cu^{II} ion. The dependences for the electron density distribution established experimentally by NMR are in good agreement with the results of theoretical calculations.[232] These data point to the presence of strong π-interaction between the $d_{x^2-y^2}$ orbital of the copper ion and the p orbital of the S atom of the cysteine residue. In addition, there exists a weaker σ-interaction between the $d_{x^2-y^2}$ orbital of the metal ion and the orbitals of the three remaining ligands.

Now we consider in more detail the hydrogen bond between the γ-S atom of the cysteine residue and the amide proton of the asparagine. It is known that this hydrogen bond is significant for the retention of the geometry of the active sites of blue proteins and their stability.[233,234] The hyperfine structure constant *a* for the amide proton of the asparagine residue and, hence, the chemical shift of the signal of this proton serves as a sensitive indicator of the strength of the hydrogen bond formed: the stronger the hydrogen bond, the higher the unpaired electron density that is transferred to the asparagine residue and the higher the absolute value of the chemical shift of this proton signal. Hence, the assignment of the amide proton of asparagine in the ^{1}H NMR spectrum of blue proteins provides information on the strength of the hydrogen bond, *i.e.*, on the distance between the NH and γ-S atoms. As found for other classes of redox proteins, hydrogen bonds play an important role in the redox potentials.[76,235–238] Further studies of blue proteins can result in establishing a correlation between the chemical shift of this amide proton and the protein redox potential.

Table 5. Separation of the contributions of various mechanisms of interaction of the unpaired electron with the ligand protons to the observed chemical shifts for oxidized plastocyanin from *Synechocystis sp.* PCC 6803 [218]

Residue	Proton	Designation in the spectrum	Cu—H /Å	δ_{obs}	δ_{dm}	δ_{dip}	δ_{cont}	*a** /MHz
His39	α-H	Z	2.9	+19.2	+6.0	+5.6	+7.6	+0.3
	β-H(1)	I	4.6	−2.7	+2.6	−0.9	−4.4	−0.2
	β-H(2)		3.2	—	—	−3.5	—	—
	δ-H(2)	B	5.2	+51.1	+7.4	−0.8	+44.5	+1.6
	ε-H(1)	E	3.1	+35.7	+7.0	−2.8	+31.5	+1.1
	N(ε-H(2))	F	5.0	+31.1	+11.7	−1.0	+20.4	+0.7
Asn40	NH	K	4.1	−15.2	+9.5	−0.7	−24.0	−0.9
	α-H	H	6.8	+14.7	+4.5	−0.1	+10.3	+0.4
Cys83	α-H	J	4.9	−7.8	+5.3	−1.1	−12.0	−0.4
	β-H(1)	X	3.2	+614	+3.5	−1.5	+612	+21.9
	β-H(2)	Y	3.4	+517	+3.0	−1.5	+516	+18.4
His86	α-H	—	5.4	—	—	−0.8	—	—
	β-H(1)	—	2.8	—	—	−3.2	—	—
	β-H(2)	—	4.1	—	—	−0.8	—	—
	δ-H(2)	A	5.2	+52.6	+7.2	−0.9	+46.3	+1.7
	ε-H(1)	D	3.2	+38.5	+7.7	−0.2	+31.0	+1.1
	N(ε-H(2))	C	5.0	+42.9	—	−0.4	—	—
Met91	α-H	—	6.6	—	—	+0.7	—	—
	β-H(1)	—	4.6	—	—	+1.7	—	—
	β-H(2)	—	4.3	—	—	+1.2	—	—
	γ-H(1)	—	4.4	—	—	+2.2	—	—
	γ-H(2)	G	4.7	+24.0	+1.5	+2.5	+20.0	+0.7
	ε–Me	—	3.9	—	—	+2.3	—	—

* *a* is the hyperfine structure constant.

Analysis of the nuclear relaxation rates in the case of plastocyanin from spinach[217] made it possible to study the contributions of the contact and dipole mechanisms to the longitudinal and transverse relaxation of various protons in the protein active site. It was found that the contact interaction between the unpaired electron and the nuclei is the prevailing type of interaction for the methylene protons of the cysteine residue and the δ-H(2) protons of the histidine residue, whereas the dipole mechanism predominates in the nuclear relaxation of the other protons.

Three-dimensional structures of a number of plastocyanins isolated from various sources have been reported.[239—254] Most of them have been determined by crystallographic analysis. This method was used to establish the structures of both the reduced and oxidized forms of plastocyanin. The structures of only the reduced form of the protein were determined by NMR.[250—254] The fact that NMR was used to study only the diamagnetic reduced form of the protein is undoubtedly related to the difficulties arising in studies of paramagnetic systems containing Cu^{2+} ions (see above).

Data on the assignment of paramagnetically shifted signals in the ^{1}H NMR spectrum of the oxidized plastocyanin from *Synechocystis sp.* PCC 6803 were used subsequently to determine the three-dimensional structure of this protein.[218] Thus, it became possible for the first time to use NMR spectroscopy for determining the conformation of the protein containing a Cu^{II} ion. This structure was constructed taking into account 1041 distance constraints obtained from analysis of the NOESY spectra, 18 distance constraints found from 1D NOE spectra, 26 metal—proton distance constraints determined from analysis of the longitudinal relaxation times for the amide protons located in the close vicinity of the copper ion, 18 hydrogen bond constraints found from analysis of the HMQC spectra in H_2O and D_2O solutions, 96 torsion angle (φ and ψ) constraints derived from the HN—HA, NOESY—HMQC, and NOESY spectra, and an angle constraint for the χ^2 torsion angle in the cysteine residue, found from analysis of the chemical shifts of the methylene signals of the cysteine residue in the ^{1}H NMR spectrum. The use of the geometric constraints resulted in a family of structures consisting of 35 conformers with RMSD values of 0.72 and 1.16 Å for the backbone and side-chain atoms, respectively. The structure of plastocyanin from *Synechocystis sp.* PCC 6803 thus obtained with elements of the secondary structure is shown in Fig. 21.[218]

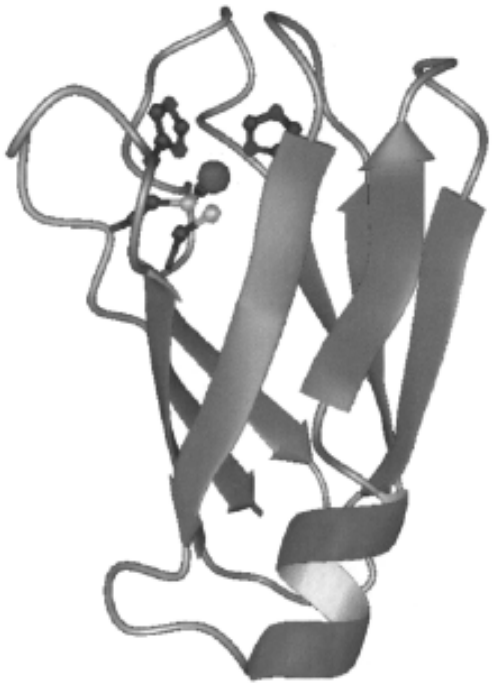

Fig. 21. Three-dimensional structure of the oxidized plastocyanin from *Synechocystis sp.* PCC 6803 in solution with elements of the protein secondary structure.

The structural and electronic investigations of blue proteins by NMR represent an important step in the development of NMR methodology because they open up the way of studying the structure, dynamics, and the functional properties of highly paramagnetic metalloproteins in solution.

Conclusion

This review considered the capacities of NMR techniques in the research of paramagnetic systems in solutions and outlined the prospects for their further development. The main procedures of structural investigation were considered for iron-sulfur and copper-containing proteins. The sequence and type of operations used for other paramagnetic systems are similar. The experiments described in this review allowed determination of the structural, functional, dynamic, and electronic characteristics of paramagnetic systems thus providing information on the biological processes involving proteins and allowed establishment of structure—function relationships controlling their activity.

The author is grateful to E. V. Dikaya for assistance in the preparation of this review.

References

1. *Nat. Struct. Biol.*, 1997, **4**, NMR special issue (suplement I).
2. *Nat. Struct. Biol.*, 1998, **5**, NMR special issue (suplement II).
3. M. P. Williamson, T. F. Havel, and K. Wüthrich, *J. Mol. Biol.*, 1985, **185**, 295.
4. R. R. Ernst, G. Bodenhausen, and A. Wokaun, *Principles of Nuclear Magnetic Resonance in one and two Dimensions*, Oxford University Press, London, 1987.
5. M. Ikura, L. E. Kay, and A. Bax, *Biochemistry,* 1990, **29**, 4659.
6. A. Bax and M. Ikura, *J. Biomol. NMR*, 1991, **1**, 99.
7. K. Pervushin, R. Riek, G. Wider, and K. Wüthrich, *Proc. Natl. Acad. Sci. USA*, 1997, **94**, 12366.
8. G. Corneliescu, J.-S. Hu, and A. Bax, *J. Am. Chem. Soc.*, 1999, **121**, 2949.

9. H. D. W. Hill, in *Encyclopedia of Nuclear Magnetic Resonance*, Eds. D. M. Grant and R. K. Harris, J. Wiley and Sons, Chichester, 1996, 3762.
10. H. D. W. Hill, in *Encyclopedia of Nuclear Magnetic Resonance*, Eds. D. M. Grant and R. K. Harris, J. Wiley and Sons, Chichester, 1996, 4505.
11. P. Bayer, L. Varani, and G. Varani, *J. Biomol. NMR*, 1999, **14**, 149.
12. G. M. Clore and A. M. Gronenborn, in *Encyclopedia of Nuclear Magnetic Resonance*, Eds. D. M. Grant and R. K. Harris, J. Wiley and Sons, Chichester, 1996, 4602.
13. L. E. Kay, *Methods Enzymol.*, 2000, **339**, 174.
14. K. Wüthrich, *Nat. Struct. Biol.*, 2000, **7**, 188.
15. K. Wüthrich, NMR *of Proteins and Nucleic Acids*, Wiley, New York, 1986.
16. L. Banci, I. Bertini, C. Luchinat, and M. Piccioli, in *NMR and Biomolecular Structure*, Eds. I. Bertini, H. Molinari, and N. Niccolai, VCH, Weinheim (Germany) 1991, 31.
17. I. Bertini, P. Turano, and A. J. Vila, *Chem. Rev.*, 1993, **93**, 2833.
18. I. Bertini and C. Luchinat, *Curr. Opin. Chem. Biol.*, 1999, **3**, 145.
19. I. Bertini, A. Rosato, and P. Turano, *Pure Appl. Chem.*, 1999, **71**, 1717.
20. G. N. La Mar, W. deW, Horrocks Jr., and R. H. Holm, *NMR of Paramagnetic Molecules*, Acad. Press, New York, 1973.
21. I. Bertini and C. Luchinat, *NMR of Paramagnetic Molecules in Biological Systems*, Benjamin/Cummings, Menlo Park, CA, 1986.
22. L. Banci, I. Bertini, and C. Luchinat, *Nuclear and Electron Relaxation. The Magnetic Nucleus-unpaired Electron Coupling in Solution*, VCH, Weinheim, 1991.
23. E. Fermi, *Z. Phys.*, 1930, **60**, 320.
24. H. M. Mc Connell and D. B. Chesnut, *J. Chem. Phys.*, 1958, **28**, 107.
25. I. Solomon, *Phys. Rev.*, 1955, **99**, 559.
26. M. Guéron, *J. Magn. Reson.*, 1975, **19**, 58.
27. A. J. Vega and D. Fiat, *Mol. Phys.*, 1976, **31**, 347.
28. M. Allegrozzi, I. Bertini, M. B. L. Janik, Y.-M. Lee, G. Liu, and C. Luchinat, *J. Am. Chem. Soc.*, 2000, **122**, 4154.
29. L. Banci, I. Bertini, and C. Luchinat, in *Methods in Enzymology*, Eds. T. L. James and N. J. Oppenheimer, Acad. Press, Inc., London, 1994, **239**, 485.
30. I. Bertini, C. Luchinat, and A. Rosato, *Progr. Biophys. Mol. Biol.*, 1996, **66**, 43.
31. I. Bertini and C. Luchinat, *Coord. Chem. Rev.*, 1996, **150**, 1.
32. L. Banci, I. Bertini, C. Luchinat, and P. Turano, in *The Porphyrin Handbook*, Eds. K. M. Kadish, K. M. Smith, and R. Guilard, Acad. Press, San Diego, CA, 2000, 323.
33. L. Banci and C. Presenti, *J. Biol. Inorg. Chem.*, 2000, **5**, 422.
34. J. S. de Ropp, P. Mandal, S. L. Brauer, and G. N. La Mar, *J. Am. Chem. Soc.*, 1997, **119**, 4732.
35. L. Banci, *J. Biotech.*, 1997, **53**, 253.
36. G. N. La Mar, Z. Chen, and J. S. de Ropp, in *Nuclear Magnetic Resonance of Paramagnetic Macromolecules*, Ed. G. N. La Mar, Kluwer Academic Publishers, Dordrecht, 1995, 55.
37. Z. G. Chen, J. S. de Ropp, G. Hernandez, and G. N. La Mar, *J. Am. Chem. Soc.*, 1994, **116**, 8772.
38. C. M. Bougault, Y. Dou, M. Ikeda-Saito, K. C. Langry, K. M. Smith, and G. N. La Mar, *J. Am. Chem. Soc.*, 1998, **120**, 2113.
39. K. Osapay, Y. Theriault, P. E. Wright, and D. A. Case, *J. Mol. Biol.*, 1994, **244**, 183.
40. Y. Yamamoto, Y. Inoue, and T. Suzuki, *Magn. Reson. Chem.*, 1993, **31**, 8.
41. G. N. La Mar, N. L. Davis, R. D. Johnson, W. S. Smith, J. B. Hauksson, D. L. Budd, F. Dalichow, K. C. Langry, I. K. Morris, and K. M. Smith, *J. Am. Chem. Soc.*, 1993, **115**, 3869.
42. I. Bertini, O. Galas, C. Luchinat, G. Parigi, and G. Spina, *J. Magn. Reson.*, 1998, **130**, 33.
43. L. Banci, I. Bertini, D. E. Cabelli, R. A. Hallewell, C. Luchinat, and M. S. Viezzoli, *Free Radical Res. Communs.*, 1991, **12—13**, 239.
44. I. Bertini, C. Luchinat, M. S. Viezzoli, and Y. Wang, *Arch. Biochem. Biophys.*, 1989, **269**, 586.
45. I. Bertini, C. Luchinat, and A. Soriano, in *Spectroscopic Methods in Bioinorganic Chemistry*, Eds. E. I. Solomon and K. O. Hodgson, ACS publications, 1998, 302.
46. I. Bertini, C. Luchinat, and A. Rosato, in *Adv. Inorg. Chem.*, Eds. A. G. Sykes and R. Cammack, Acad. Press, San Diego, 1999, 251.
47. I. Bertini, M. Piccioli, A. Scozzafava, and M. S. Viezzoli, *Magn. Reson. Chem.*, 1993, **31**, S17.
48. L. Banci, I. Bertini, C. Luchinat, M. S. Viezzoli, and Y. Wang, *Inorg. Chem.*, 1988, **27**, 1442.
49. Z. Wang, L.-J. Ming, L. Que, Jr., J. B. Vincent, M. W. Crowder, and B. A. Averill, *Biochemistry*, 1992, **31**, 5263.
50. I. Moura, M. Teixeira, J. LeGall, and J. J. G. Moura, *J. Inorg. Biochem.*, 1991, **44**, 127.
51. I. Bertini, K. L. Bren, A. Clemente, J. A. Fee, H. B. Gray, C. Luchinat, B. G. Malmström, J. H. Richards, D. Sanders, and C. E. Slutter, *J. Am. Chem. Soc.*, 1996, **46**, 11658.
52. J. Salgado, G. Warmerdam, L. Bubacco, and G. W. Canters, *Biochemistry*, 1998, **37**, 7378.
53. C. Dennison, A. Berg, and G. W. Canters, *Biochemistry*, 1997, **36**, 3262.
54. C. Dennison, A. Berg, S. de Vries, and G. W. Canters, *FEBS Lett.*, 1996, **394**, 340.
55. *Advances in Inorganic Chemistry. Iron Sulfur Proteins*, Eds. R. Cammack and A. G. Sykes, Acad. Press., San Diego, 1992.
56. J. B. Howard and D. C. Rees, *Adv. Prot. Chem.*, 1991, **42**, 199.
57. A. J. Thompson, in *Metalloproteins*, Ed. P. Harrison, Verlag Chemie, Weinheim, FRG, 1985, 79.
58. H. Beinert, *Federation of Am. Soc. for Experimental Biol. J.*, 1990, **4**, 2483.
59. H. Beinert, R. H. Holm, and E. Münck, *Science*, 1997, **277**, 653.
60. R. J. Gurbiel, T. Ohnishi, D. E. Robertson, F. Daldal, and B. M. Hoffman, *Biochemistry,* 1991, **30**, 11579.
61. R. J. Gurbiel, C. J. Batie, M. Sivaraja, A. E. True, J. A. Fee, B. M. Hoffman, and D. P. Ballou, *Biochemistry*, 1989, **28**, 4861.
62. H. Beinert, M. C. Kennedy, and C. D. Stout, *Chem. Rev.* 1996, **96**, 2335.
63. M. M. Werst, M. C. Kennedy, H. Beinert, and B. M. Hoffman, *Biochemistry,* 1990, **29**, 10526.
64. S. J. George, F. A. Armstrong, E. C. Hatchikian, and A. J. Thompson, *Biochem. J.*, 1989, **264**, 275.
65. R. C. Conover, A. T. Kowal, W. Fu, J.-B. Park, S. Aono, M. W. W. Adams, and M. K. Johnson, *J. Biol. Chem.*, 1990, **265**, 8533.
66. M. De Vocht, I. M. Kooter, Y. B. M. Bulsink, W. R. Hagen, and M. K. Johnson, *J. Am. Chem. Soc.* 1996, **118**, 2766.

67. W. R. Rypniewski, D. R. Breiter, M. M. Benning, G. Wesenberg, B.-H. Oh, J. L. Markley, I. Rayment, and H. M. Holden, *Biochemistry*, 1991, **30**, 4126.
68. K. Fukuyama, T. Hase, S. Matsumoto, T. Tsukihara, and Y. Katsube, *Nature,* 1980, **286**, 522.
69. T. Tsukihara, K. Fukuyama, M. Nakamura, Y. Katsube, N. Tanaka, M. Kakudo, K. Wasa, T. Hase, and H. Matsubara, *J. Biochem.*, 1981, **90**, 1763.
70. C. W. J. Carter, J. Kraut, S. T. Freer, and R. A. Alden, *J. Biol. Chem.*, 1974, **249**, 6339.
71. C. W. J. Carter, in *Iron-Sulfur Protein*, Ed. W. Lovenberg, Acad. Press, New York, 1977, 157.
72. D. R. Breiter, T. E. Meyer, I. Rayment, and H. M. Holden, *J. Biol. Chem.*, 1991, **266**, 18660.
73. C. R. Kissinger, E. T. Adman, L. C. Sieker, and L. H. Jensen, *J. Am. Chem. Soc.*, 1988, **110**, 8721.
74. C. R. Kissinger, E. T. Adman, L. C. Sieker, L. H. Jensen, and J. LeGall, *FEBS Lett.*, 1989, **244**, 447.
75. H. Matsubara and K. Saeki, *Adv. Inorg. Chem.*, 1992, **38**, 223.
76. G. Backes, Y. Mino, T. M. Loehr, T. E. Meyer, M. A. Cusanovich, W. V. Sweeney, E. T. Adman, and J. Sanders-Loehr, *J. Am. Chem. Soc.*, 1991, **113**, 2055.
77. K. Fukuyama, Y. Nagahara, T. Tsukihara, and Y. Katsube, *J. Mol. Biol.*, 1988, **199**, 183.
78. K. Fukuyama, Y. Nagahara, T. Tsukihara, and Y. Katsube, *J. Mol. Biol.*, 1989, **210**, 383.
79. C. R. Kissinger, L. C. Sieker, E. T. Adman, and L. H. Jensen, *J. Mol. Biol.*, 1991, **219**, 693.
80. H. M. KrishnaMurthy, W. A. Hendrickson, W. H. Orme-Johnson, E. A. Merritt, and R. P. Phizackerley, *J. Biol. Chem.*, 1988, **263**, 18430.
81. C. D. Stout, *J. Mol. Biol.*, 1989, **205**, 545.
82. E. T. Adman, L. C. Sieker, and L. H. Jensen, *J. Biol. Chem.*, 1973, **248**, 3987.
83. E. T. Adman, L. C. Sieker, and L. H. Jensen, *J. Biol. Chem.*, 1976, **251**, 3801.
84. W. R. Hagen, A. J. Pierik, and C. Veeger, *J. Chem. Soc., Faraday Trans.*, 1989, **85**, 4083.
85. A. J. Pierik, R. B. G. Wolbert, P. H. A. Mutsaers, W. R. Hagen, and C. Veeger, *Eur. J. Biochem.*, 1992, **206**, 697.
86. J. M. Berg, R. H. Holm, in *Iron-Sulfur Proteins*, Ed. T. G. Spiro, Wiley-Interscience, New York, 1982, 1.
87. L. Banci, I. Bertini, A. Dikiy, D. H. W. Kastrau, C. Luchinat, and P. Sompornpisut, *Biochemistry,* 1995, **34**, 206.
88. I. Bertini, A. Dikiy, D. H. W. Kastrau, C. Luchinat, and P. Sompornpisut, *Biochemistry,* 1995, **34**, 9851.
89. L. Banci, I. Bertini, L. D. Eltis, I. C. Felli, D. H. W. Kastrau, C. Luchinat, M. Piccioli, R. Pierattelli, and M. Smith, *Eur. J. Biochem.*, 1994, **225**, 715.
90. K. D. Watenpaugh, L. C. Sieker, and L. H. Jensen, *J. Mol. Biol.*, 1979, **131**, 509.
91. R. E. Stenkamp, L. C. Sieker, and L. H. Jensen, *Proteins Struct. Funct. Genet.*, 1990, **8**, 352.
92. M. Bruschi, I. Moura, J. LeGall, A. V. Xavier, and L. C. Sieker, *Biochem. Biophys. Res. Commun.*, 1979, **90**, 596.
93. L. Yu, M. Kennedy, C. Czaja, P. Tavares, J. J. G. Moura, I. Moura, and F. M. Rusnak, *Biochem. Biophys. Res. Commun.*, 1997, **231**, 679.
94. I. Moura, P. Tavares, J. J. G. Moura, N. Ravi, B. H. Huynh, M.-Y. Liu, and J. LeGall, *J. Biol. Chem.*, 1990, **265**, 21596.
95. J. LeGall, B. C. Prickril, I. Moura, A. V. Xavier, J. J. G. Moura, and B. H. Huynh, *Biochemistry*, 1988, **27**, 1636.
96. V. S. Shenoy and T. Ichiye, *Proteins Struct. Funct. Genet.*, 1993, **17**, 152.
97. R. Krishnamoorthi, J. L. Markley, M. A. Cusanovich, and C. T. Przysiecki, *Biochemistry*, 1986, **25**, 50.
98. M. T. Werth, D. M. Kurtz, Jr., I. Moura, and J. LeGall, *J. Am. Chem. Soc.*, 1987, **109**, 273.
99. P. R. Blake, J.-B. Park, F. O. Bryant, S. Aono, J. K. Magnuson, E. Eccleston, J. B. Howard, M. F. Summers, and M. W. W. Adams, *Biochemistry*, 1991, **30**, 10885.
100. I. Bertini, D. M. Kurtz, Jr., M. K. Eidsness, G. Liu, C. Luchinat, A. Rosato, and R. A. Scott, *J. Biol. Inorg. Chem.*, 1998, **3**, 401.
101. B. Xia, W. M. Westler, H. Cheng, J. Meyer, J.-M. Moulis, and J. L. Markley, *J. Am. Chem. Soc.*, 1995, **117**, 5347.
102. S. J. Wilkens, B. Xia, F. Weinhold, J. L. Markley, and W. M. Westler, *J. Am. Chem. Soc.*, 1998, **120**, 4806.
103. D. C. Yoch and R. P. Carithers, *Microbiol. Rev.*, 1979, **43**, 384.
104. F. A. Armstrong, S. J. George, A. J. Thomson, and M. G. Yates, *FEBS Lett.*, 1988, **234**, 107.
105. A. Abragam, *The Principles of Nuclear Magnetism*, Oxford University Press, Oxford, 1961,
106. L. Banci, I. Bertini, and C. Luchinat, *Struct. Bonding*, 1990, **72**, 113.
107. M. Poe, W. D. Phillips, C. C. McDonald, and W. Lovenberg, *Proc. Natl. Acad. Sci. USA*, 1970, **65**, 797.
108. L. B. Dugad, G. N. La Mar, L. Banci, and I. Bertini, *Biochemistry,* 1990, **29**, 2263.
109. L. Skjeldal, W. M. Westler, and J. L. Markley, *Arch. Biochem. Biophys.*, 1990, **278**, 482.
110. I. Salmeen and G. Palmer, *Arch. Biochem. Biophys.*, 1972, **150**, 767.
111. J. D. Glickson, W. D. Phillips, C. C. McDonald, and M. Poe, *Biochem. Biophys. Res. Commun.*, 1971, **42**, 271.
112. W. D. Phillips, C. C. McDonald, N. A. Stombaugh, and W. H. Orme-Johnson, *Proc. Natl. Acad. Sci. USA*, 1974, **71**, 140.
113. L. Skjeldal, J. L. Markley, V. M. Coghlan, and L. E. Vickery, *Biochemistry,* 1991, **30**, 9078.
114. R. Miura and Y. Ichikawa, *J. Biol. Chem.*, 1991, **266**, 6252.
115. I. Bertini, G. Lanini, and C. Luchinat, *Inorg. Chem.*, 1984, **23**, 2729.
116. W. R. Dunham, G. Palmer, R. H. Sands, and A. J. Bearden, *Biochim. Biophys. Acta*, 1971, **253**, 373.
117. G. Palmer, W. R. Dunham, J. A. Fee, R. H. Sands, T. Izuka, and T. Yonetani, *Biochim. Biophys. Ac*ta, 1971, **2**45, 201.
118. C. Lelong, P. Sétif, H. Bottin, F. André, and J.-M. Neumann, *Biochemistry*, 1995, **34**, 14462.
119. H. Hatanaka, R. Tanimura, S. Katoh, and F. Inagaki, *J. Mol. Biol.*, 1997, **268**, 922.
120. B. Baumann, H. Sticht, M. Schärpf, M. Sutter, W. Haehnel, and P. Roesch, *Biochemistry*, 1996, **35**, 12831.
121. S.-C. Im, G. Liu, C. Luchinat, A. G. Sykes, and I. Bertini, *Eur. J. Biochem.*, 1998, **258**, 465.
122. T. C. Pochapsky, X. M. Ye, G. Ratnaswamy, and T. A. Lyons, *Biochemistry*, 1994, **33**, 6424.
123. T. C. Pochapsky, N. U. Jain, M. Kuti, T. A. Lyons, and J. Heymont, *Biochemistry*, 1999, **38**, 4681.
124. A. V. Xavier, J. J. G. Moura, and I. Moura, *Struct. Bonding*, 1981, **43**, 187.
125. M. H. Emptage, T. A. Kent, B. H. Huynh, J. Rawlings, W. H. Orme-Johnson, and E. Münck, *J. Biol. Chem.*, 1980, **255**, 1793.

126. M. C. Kennedy and C. D. Stout, *Adv. Inorg. Chem.*, 1992, **38**, 323.
127. A. H. Robbins and C. D. Stout, *Proc. Natl. Acad. Sci. USA*, 1989, **86**, 3639.
128. T. A. Kent, B. H. Huynh, and E. Munk, *Proc. Natl. Acad. Sci. USA*, 1980, **77**, 6574.
129. J.-P. Gayda, P. Bertrand, F. X. Theodule, and J. J. G. Moura, *J. Chem. Phys.*, 1982, **77**, 3387.
130. A. L. Macedo, I. Moura, J. J. G. Moura, J. LeGall, and B. H. Huynh, *Inorg. Chem.*, 1993, **32**, 1101.
131. S. C. Busse, G. N. La Mar, L. P. Yu, J. B. Howard, E. T. Smith, Z. H. Zhou, and M. W. W. Adams, *Biochemistry*, 1992, **31**, 11952.
132. A. Donaire, C. M. Gorst, Z. H. Zhou, M. W. W. Adams, and G. N. La Mar, *J. Am. Chem. Soc.*, 1994, **116**, 6841.
133. C. M. Gorst, Y. H. Yeh, Q. Teng, L. Calzolai, Z. H. Zhou, M. W. M. Adams, and G. N. La Mar, *Biochemistry*, 1995, **34**, 600.
134. A. L. Macedo, P. N. Palma, I. Moura, J. LeGall, V. Wray, and J. J. G. Moura, *Magn. Reson. Chem.*, 1993, **31**, S59.
135. I. Bertini, S. Ciurli, and C. Luchinat, *Struct. Bonding*, 1995, **83**, 1.
136. B. J. Goodfellow, A. L. Macedo, P. Rodrigues, I. Moura, V. Wray, and J. J. G. Moura, *J. Biol. Inorg. Chem.*, 1999, **4**, 421.
137. C. W. J. Carter, J. Kraut, S. T. Freer, R. A. Alden, L. C. Sieker, E. T. Adman, and L. H. Jensen, *Proc. Natl. Acad. Sci. USA*, 1972, **69**, 3526.
138. M. Poe, W. D. Phillips, J. D. Glickson, C. C. McDonald, and A. San Pietro, *Proc. Natl. Acad. Sci. USA*, 1971, **68**, 68.
139. W. D. Phillips, M. Poe, C. C. McDonald, and R. G. Bartsch, *Proc. Natl. Acad. Sci. USA*, 1970, **67**, 682.
140. I. Bertini, F. Briganti, C. Luchinat, and A. Scozzafava, *Inorg. Chem.*, 1990, **29**, 1874.
141. I. Bertini, F. Briganti, C. Luchinat, L. Messori, R. Monnanni, A. Scozzafava, and G. Vallini, *FEBS Lett.*, 1991, **289**, 253.
142. E. L. Packer, W. V. Sweeney, J. C. Rabinowitz, H. Sternlicht, and E. N. Shaw, *J. Biol. Chem.*, 1977, **252**, 2245.
143. S. C. Busse, G. N. La Mar, and J. B. Howard, *J. Biol. Chem.*, 1991, **266**, 23714.
144. J. Gaillard, J.-M. Moulis, R. Kummerle, and J. Meyer, *Magn. Reson. Chem.*, 1993, **31**, S27.
145. J. G. Huber, J. Gaillard, and J.-M. Moulis, *Biochemistry*, 1995, **34**, 194.
146. P. Kyritsis, R. Kummerle, J. G. Huber, J. Gaillard, B. Guigliarelli, C. Popescu, E. Munck, and J.-M. Moulis, *Biochemistry*, 1999, **38**, 6335.
147. I. Bertini, A. Donaire, B. A. Feinberg, C. Luchinat, M. Piccioli, and H. Yuan, *Eur. J. Biochem.*, 1995, **232**, 192.
148. I. Bertini, F. Capozzi, C. Luchinat, M. Piccioli, and A. J. Vila, *J. Am. Chem. Soc.*, 1994, **116**, 651.
149. D. Bentrop, I. Bertini, C. Luchinat, J. Mendes, M. Piccioli, and M. Teixeira, *Eur. J. Biochem.*, 1996, **236**, 92.
150. A. Donaire, Z. H. Zhou, M. W. W. Adams, and G. N. La Mar, *J. Biomol. NMR*, 1996, **7**, 35.
151. P. L. Wang, A. Donaire, Z. H. Zhou, M. W. W. Adams, and G. N. La Mar, *Biochemistry*, 1996, **35**, 11319.
152. J.-M. Moulis, P. Auric, J. Gaillard, and J. Meyer, *J. Biol. Chem.*, 1984, **259**, 11396.
153. K. Gersonde, H.-E. Schlaak, M. Breitenbach, F. Parak, H. Eicher, W. Zgorzalla, M. G. Kalvius, and A. Mayer, *Eur. J. Biochem.*, 1974, **43**, 307.
154. J. Gaillard, J.-P. Albrand, J.-M. Moulis, and D. E. Wemmer, *Biochemistry*, 1992, **31**, 5632.
155. I. Bertini, F. Briganti, C. Luchinat, L. Messori, R. Monnanni, A. Scozzafava, and G. Vallini, *Eur. J. Biochem.*, 1992, **204**, 831.
156. E. L. Packer, H. Sternlicht, E. T. Lode, and J. C. Rabinowitz, *J. Biol. Chem.*, 1975, **250**, 2062.
157. H. Sticht, G. Wildegger, D. Bentrop, B. Darimont, R. Sterner, and P. Roesch, *Eur. J. Biochem.*, 1996, **237**, 726.
158. S. L. Davy, M. J. Osborne, and G. R. Moore, *J. Mol. Biol.*, 1998, **277**, 683.
159. G. Battistuzzi, M. Borsari, S. Ferretti, C. Luchinat, and M. Sola, *Arch. Biochem. Biophys.*, 1995, **320**, 149.
160. K. Nagayama, D. Ohmori, Y. Imai, and T. Oshima, *FEBS Lett.*, 1983, **158**, 208.
161. K. Nagayama and D. Ohmori, *FEBS Lett.*, 1984, **173**, 15.
162. K. Nagayama, Y. Imai, D. Ohmori, and T. Oshima, *FEBS Lett.*, 1984, **169**, 79.
163. M. K. Johnson, D. E. Bennett, J. A. Fee, and W. V. Sweeney, *Biochim. Biophys. Acta*, 1987, **911**, 81.
164. H. Cheng, K. Grohmann, and W. V. Sweeney, *J. Biol. Chem.*, 1990, **265**, 12388.
165. H. Cheng, K. Grohmann, and W. V. Sweeney, *J. Biol. Chem.*, 1992, **267**, 8073.
166. S. Aono, I. Bertini, J. A. Cowan, C. Luchinat, A. Rosato, and M. S. Viezzoli, *J. Biol. Inorg. Chem.*, 1996, **1**, 523.
167. I. Bertini, A. Dikiy, C. Luchinat, R. Macinai, M. S. Viezzoli, and M. Vincenzini, *Biochemistry*, 1997, **36**, 3570.
168. S. Aono, D. Bentrop, I. Bertini, A. Donaire, C. Luchinat, Y. Niikura, and A. Rosato, *Biochemistry*, 1998, **37**, 9812.
169. S. Aono, D. Bentrop, I. Bertini, G. Cosenza, and C. Luchinat, *Eur. J. Biochem.*, 1998, **258**, 502.
170. R. Cammack, *Adv. Inorg. Chem.*, 1992, **38**, 281.
171. T. E. Meyer, C. T. Przysiecki, J. A. Watkins, A. Bhattacharyya, R. P. Simondsen, M. A. Cusanovich, and G. Tollin, *Proc. Natl. Acad. Sci. USA*, 1983, **80**, 6740.
172. P. Middleton, D. P. E. Dickson, C. E. Johnson, and J. D. Rush, *Eur. J. Biochem.*, 1980, **104**, 289.
173. I. Bertini, A. P. Campos, C. Luchinat, and M. Teixeira, *J. Inorg. Biochem.*, 1993, **52**, 227.
174. B. C. Antanaitis and T. H. Moss, *Biochim. Biophys. Acta*, 1975, **405**, 262.
175. J. D. Rush, W. H. Koppenol, E. A. E. Garber, and E. Margoliash, *J. Biol. Chem.*, 1988, **263**, 7514.
176. I. Bertini, F. Briganti, C. Luchinat, A. Scozzafava, and M. Sola, *J. Am. Chem. Soc.*, 1991, **113**, 1237.
177. L. Banci, I. Bertini, F. Briganti, C. Luchinat, A. Scozzafava, and M. Vicens Oliver, *Inorg. Chem.*, 1991, **30**, 4517.
178. (a) L. Banci, I. Bertini, F. Capozzi, P. Carloni, S. Ciurli, C. Luchinat, and M. Piccioli, *J. Am. Chem. Soc.*, 1993, **115**, 3431; (b) I. Bertini, F. Capozzi, C. Luchinat, and M. Piccioli, *Eur. J. Biochem.*, 1993, **212**, 69; (c) I. Bertini, F. Capozzi, C. Luchinat, M. Piccioli, and M. Vicens Oliver, *Inorg. Chim. Acta*, 1992, **198—200**, 483; (d) S. Ciurli, M. A. Cremonini, P. Kofod, and C. Luchinat, *Eur. J. Biochem.*, 1996, **236**, 405.
179. E. Babini, I. Bertini, M. Borsari, F. Capozzi, A. Dikiy, L. D. Eltis, and C. Luchinat, *J. Am. Chem. Soc.*, 1996, **118**, 75.
180. I. Bertini, F. Capozzi, S. Ciurli, C. Luchinat, L. Messori, and M. Piccioli, *J. Am. Chem. Soc.*, 1992, **114**, 3332.
181. L. Banci, I. Bertini, S. Ciurli, S. Ferretti, C. Luchinat, and M. Piccioli, *Biochemistry*, 1993, **32**, 9387.

182. R. Krishnamoorthi, J. L. Markley, M. A. Cusanovich, C. T. Przysiecki, and T. E. Meyer, *Biochemistry*, 1986, **25**, 60.
183. I. Bertini, A. Gaudemer, C. Luchinat, and M. Piccioli, *Biochemistry*, 1993, **32**, 12887.
184. O. Jardetzky, G. C. K. Robert, in *NMR in Molecular Biology*, Anonymous, Acad. Press, New York, 1981.
185. I. Bertini, L. D. Eltis, I. C. Felli, D. H. W. Kastrau, C. Luchinat, and M. Piccioli, *Chemistry — A European Journal*, 1995, **1**, 598.
186. D. Bentrop, I. Bertini, F. Capozzi, A. Dikiy, L. D. Eltis, and C. Luchinat, *Biochemistry*, 1996, **35**, 5928.
187. A. Arseniev, P. Schultze, E. Wörgötter, W. Braun, G. Wagner, M. Vasak, J. H. Kägi, and K. Wüthrich, *J. Mol. Biol.*, 1988, **201**, 637.
188. P. Schultze, E. Wörgötter, W. Braun, G. Wagner, M. Vasak, J. H. Kägi, and K. Wüthrich, *J. Mol. Biol.*, 1988, **203**, 251.
189. I. Bertini, A. Dikiy, C. Luchinat, M. Piccioli, and D. Tarchi, *J. Magn. Reson. Ser. B*, 1994, **103**, 278.
190. I. Bertini, M. M. J. Couture, A. Donaire, L. D. Eltis, I. C. Felli, C. Luchinat, M. Piccioli, and A. Rosato, *Eur. J. Biochem.*, 1996, **241**, 440.
191. P. Güntert, W. Braun, and K. Wüthrich, *J. Mol. Biol.*, 1991, **217**, 517.
192. D. A. Pearlman, D. A. Case, G. C. Caldwell, G. L. Siebel, U. C. Singh, P. Weiner, and P. A. Kollman, *AMBER 4.0*, University of California, San Francisco, 1991.
193. J. J. R. Frausto da Silva and R. J. P. Williams, *The Biological Chemistry of the Elements*, Oxford, 1991.
194. R. Malkin and B. G. Malmstrцm, *Adv. Enzymol.*, 1970, 177.
195. A. Messerschmidt, *Struct. Bonding*, 1998, **90**, 37.
196. E. T. Adman, *Adv. Prot. Chem.*, 1991, **42**, 144.
197. A. G. Sykes, *Adv. Inorg. Chem.*, 1991, 377.
198. B. G. Malmstrцm, *Eur. J. Biochem.*, 1994, **223**, 711.
199. A. Messerschmidt, *Multicopper Oxidases*, World Scientific, River Edje, N. J., 1997.
200. H. B. Gray, B. G. Malmstrцm, and R. J. Williams, *J. Biol. Inorg. Chem.*, 2000, **5**, 551.
201. J. A. Guckert, M. D. Lowery, and E. I. Solomon, *J. Am. Chem. Soc.*, 1995, **115**, 2817.
202. H. B. Gray and B. G. Malmstrцm, *Comments Inorg. Chem.*, 1983, **2**, 203.
203. A. J. Vila, *FEBS Lett.*, 1994, **355**, 15.
204. M. V. Botuyan, A. Toy-Palmer, J. Chung, R. C. Blake, P. Beroza, D. A. Case, and H. J. Dyson, *J. Mol. Biol.*, 1996, **263**, 752.
205. D. R. McMillin, R. A. Holwerda, and H. B. Gray, *Proc. Natl. Acad. Sci. USA*, 1974, **71**, 1339.
206. D. R. McMillin, R. C. Rosenberg, and H. B. Gray, *Proc. Natl. Acad. Sci. USA*, 1974, **71**, 4760.
207. K. W. Penfield, A. A. Gewirth, and E. I. Solomon, *J. Am. Chem. Soc.*, 1985, **107**, 4519.
208. L. Ryden and L. T. Hunt, *J. Mol. Evol.*, 1993, **36**, 41.
209. L. Ryden, in *Copper Proteins and Copper Enzymes*, *Vol. II*, Ed. R. Lontie, CRC Press, Boca Raton, 2000, 207.
210. J. P. Hart, A. M. Nersissian, R. G. Herrmann, R. M. Nalbandyan, J. S. Valentine, and D. Eisenberg, *Protein Sci.*, 1996, **5**, 2175.
211. V. Ducros, A. M. Brzozowski, K. S. Wilson, S. H. Brown, P. Ostergaard, P. Schneider, D. S. Yaver, A. H. Pedersen, and G. J. Davies, *Nature Struct. Biol.*, 1998, **5**, 310.
212. A. P. Kalverda, J. Salgado, C. Dennison, and G. W. Canters, *Biochemistry*, 1996, **35**, 3092.
213. C. O. Fernandez, A. I. Sannazzaro, and A. J. Vila, *Biochemistry*, 1997, **36**, 10566.
214. A. J. Vila, B. E. Ramirez, A. J. Di Bilio, T. J. Mizoguchi, J. H. Richards, and H. B. Gray, *Inorg. Chem.*, 1997, **36**, 4567.
215. J. Salgado, S. J. Kroes, A. Berg, J. M. Moratal, and G. W. Canters, *J. Biol. Chem.*, 1998, **273**, 177.
216. C. Dennison and T. Kohzuma, *Inorg. Chem.*, 1999, **38**, 1491.
217. I. Bertini, S. Ciurli, A. Dikiy, R. Gasanov, C. Luchinat, G. Martini, and N. Safarov, *J. Am. Chem. Soc.*, 1999, **121**, 2037.
218. I. Bertini, S. Ciurli, A. Dikiy, C. O. Fernández, C. Luchinat, N. Safarov, S. Shumilin, and A. J. Vila, *J. Am. Chem. Soc.*, 2001, **123**, 2405.
219. I. Bertini, C. O. Fernández, B. G. Karlsson, J. Leckner, C. Luchinat, B. G. Malmström, A. M. Nersissian, R. Pierattelli, E. Shipp, J. S. Valentine, and A. J. Vila, *J. Am. Chem. Soc.*, 2000, **122**, 3701.
220. M. R. Redinbo, T. O. Yeates, and S. Merchant, *J. Bioenerg. Biomemb.*, 1994, **26**, 49.
221. J. A. Navarro, M. Hervбs, and M. A. De la Rosa, *J. Biol. Inorg. Chem.*, 1994, **2**, 11.
222. A. B. Hope, *Biochim. Biophys. Acta*, 2000, **1456**, 5.
223. I. Bertini, D. A. Bryant, S. Ciurli, A. Dikiy, C. O. Fernández, C. Luchinat, N. Safarov, S. Shumilin, A. J. Vila, and J. Zhao, *J. Biol. Chem.*, 2001, **276**, 47217.
224. P. Kyritsis, C. Dennison, W. J. Ingledew, W. McFarlane, and A. G. Sykes, *Inorg. Chem.*, 1995, **34**, 5370.
225. M. M. Werst, E. E. Davoust, and B. M. Hoffman, *J. Am. Chem. Soc.*, 1991, **113**, 1533.
226. S. E. Shadle, J. E. Penner-Hahn, H. J. Schugar, B. Hedman, K. O. Hodgson, and E. I. Solomon, *J. Am. Chem. Soc.*, 1993, **115**, 767.
227. S. J. George, M. D. Lowery, E. I. Solomon, and W. A. Cramer, *J. Am. Chem. Soc.*, 1993, **115**, 2968.
228. G. N. La Mar, W. deW., Horrocks Jr., and R. H. Holm, *NMR of Paramagnetic Molecules*, Acad. Press, New York, 1973.
229. H. M. McConnell and D. B. Chesnut, *J. Chem. Phys.*, 1958, **28**, 107.
230. C. G. Holmberg and C. B. Laurell, *Acta Chem. Scand.*, 1948, **2**, 550.
231. J. E. Roberts, J. F. Cliine, V. Lum, H. Freeman, H. B. Gray, J. Peisach, B. Reinhammar, and B. M. Hoffman, *J. Am. Chem. Soc.*, 1984, **106**, 5324.
232. A. A. Gewirth and E. I. Solomon, *J. Am. Chem. Soc.*, 1988, **110**, 3811.
233. C. W. Hoitink and G. W. Canters, *J. Biol. Chem.*, 1992, **267**, 13836.
234. S. Dong, J. A. Ybe, M. H. Hecht, and T. G. Spiro, *Biochemistry*, 1999, **38**, 3379.
235. L. Banci, I. Bertini, S. Ciurli, C. Luchinat, and R. Pierattelli, *Inorg. Chim. Acta*, 1995, **240**, 251.
236. R. Langen, G. M. Jensen, U. Jacob, P. J. Stephen, and A. Warshel, *J. Biol. Chem.*, 1992, **267**, 25625.
237. A. K. Churg, A. Warshel, *Biochemistry*, 1986, **25**, 1675.
238. E. T. Adman, K. D. Watenpaugh, and L. H. Jensen, *Proc. Natl. Acad. Sci. USA*, 1975, **72**, 4845.
239. J. M. Guss, P. R. Harrowell, M. Murata, V. A. Norris, and H. C. Freeman, *J. Mol. Biol.*, 1986, **192**, 361.
240. J. M. Guss, H. D. Bartunik, and H. C. Freeman, *Acta Cryst.*, 1992, **B48**, 790.

241. Collyer, C. A., J. M. Guss, Y. Sugimura, F. Yoshizaki, and H. C. Freeman, *J. Mol. Biol.*, 1990, **211**, 617.
242. M. R. Redinbo, D. Cascio, M. K. Choukair, D. Rice, S. Merchant, and T. O. Yeates, *Biochemistry*, 1993, **32**, 10560.
243. N. Shibata, T. Inoue, C. Nagano, N. Nishio, T. Kohzuma, K. Onodera, F. Yoshizaki, Y. Sugimura, and Y. Kai, *J. Biol. Chem.*, 1999, **274**, 4225.
244. A. Romero, B. De la Cerda, P. F. Vareda, J. A. Navarro, M. Hervás, and M. A. De la Rosa, *J. Mol. Biol.*, 1998, **275**, 327.
245. Y. Xue, M. Okvist, O. Hansson, and S. Young, *Protein Sci.*, 1998, **7**, 2099.
246. C. S. Bond, D. S. Bendall, H. C. Freeman, J. M. Guss, C. J. Howe, M. J. Wagner, and M. C. Wilce, *Acta Crystallogr. D, Biol. Crystallogr.*, 1999, **55** (Pt 2), 414.
247. T. Inoue, M. Gotowda, H. Sugawara, H. Kohzuma, F. Yoshizaki, Y. Sugimura, and Y. Kai, *Biochemistry*, 1999, **38**, 13853.
248. T. Inoue, H. Sugawara, S. Hamanaka, H. Tsukui, E. Suzuki, H. Kohzuma, and Y. Kai, *Biochemistry*, 1999, **38**, 6063.
249. H. Sugawara, T. Inoue, C. Li, M. Gotowda, T. Hibino, T. Takabe, and Y. Kai, *J. Biochem. (Tokyo)*, 1999, **125**, 899.
250. U. Badsberg, A. M. Jorgensen, H. Gesmar, J. J. Led, J. M. Hammerstad, L. L. Jespersen, and J. Ulstrup, *Biochemistry*, 1996, **35**, 7021.
251. C. R. Babu, B. F. Volkman, and G. S. Bullerjahn, *Biochemistry*, 1999, **38**, 4988.
252. J. M. Moore, C. A. Lepre, G. P. Gippert, W. J. Chazin, D. A. Case, and P. E. Wright, *J. Mol. Bi*ol., 1991, **2**21, 533.
253. S. Bagby, P. C. Driscoll, T. S. Harvey, and H. A. O. Hill, *Biochemistry*, 1994, **33**, 6611.
254. L. Ma, A. M. M. Jørgensen, G. O. Sorensen, J. Ulstrup, and J. J. Led, *J. Am. Chem. Soc.*, 2000, **122**, 9473.

Received April 3, 2001